

Quantum statistical mechanics of encryption: reaching the speed limit of classical block ciphers

Claudio Chamon,¹ Eduardo R. Mucciolo,² and Andrei E. Ruckenstein¹

¹*Physics Department, Boston University, Boston, Massachusetts 02215, USA*

²*Department of Physics, University of Central Florida, Orlando, Florida 32816, USA*

(Dated: March 8, 2022)

We cast encryption via classical block ciphers in terms of operator spreading in a dual space of Pauli strings, a formulation which allows us to characterize classical ciphers by using tools well known in the analysis of quantum many-body systems. We connect plaintext and ciphertext attacks to out-of-time order correlators (OTOCs) and quantify the quality of ciphers using measures of delocalization in string space such as participation ratios and corresponding entropies obtained from the wave function amplitudes in string space. In particular, we show that in Feistel ciphers the entropy saturates its bound to exponential precision for ciphers with 4 or more rounds, consistent with the classic Luby-Rackoff result that it takes these many rounds to generate strong pseudorandom permutations. The saturation of the string-space information entropy is accompanied by the vanishing of OTOCs. Together these signal irreversibility and chaos, which we take to be the defining properties of good classical ciphers. More precisely, we define a good cipher by requiring that the OTOCs vanish to exponential precision and that the string entropies saturate to the values associated with a random permutation, which are computed explicitly in the paper. In turn, these criteria imply that the cipher cannot be distinguished from a pseudorandom permutation with a polynomial number of queries. We argue that the conditions on both OTOCs and string entropies can be satisfied by n -bit block ciphers implemented via random reversible circuits with $\mathcal{O}(n \log n)$ gates. This paper focuses on a tree-structured cipher composed of layers of $n/3$ 3-bit gates, for which a “key” specifies uniquely the sequence of gates that comprise the circuit. We show that in order to reach this “speed limit” one must employ a three-stage circuit consisting of a nonlinear stage implemented by layers of nonlinear gates that proliferate the number of strings, flanked by two linear stages, each deploying layers of a special set of linear “inflationary” gates that accelerate the growth of small individual strings. The close formal correspondence to quantum scramblers established in this work leads us to suggest that this three-stage construction is also required in order to scramble quantum states to similar precision and with circuits of similar size. A shallow, $\mathcal{O}(\log n)$ -depth cipher of the type described here can be used in constructing a polynomial-overhead scheme for computation on encrypted data proposed in another publication as an alternative to Homomorphic Encryption.

I. INTRODUCTION

A block cipher encrypts a plaintext message, broken up into a series of blocks of bits, by mapping it into ciphertext blocks of the same size [1]. The development of algorithms that implement “good” block ciphers usually involves constructing pseudorandom permutations through an iterative process which scrambles the initial plaintext. Notable examples are: (1) Feistel ciphers [1, 2], which use pseudorandom functions to build pseudorandom permutations through multiple rounds of shuffles and toggles of bit-registers; and (2) random compositions of small permutations on, at a minimum, 3 bits at a time [3–5]. In this paper we use the latter framework of random classical circuits built from universal 3-bit gates to explore classical ciphers from a new point of view. In particular, we formulate plaintext or ciphertext attacks, which can be cast as combinations of flipping and/or measuring strings of bits, in terms of out-of-time-order correlators (OTOCs) of string operators representing the attacks. In our specific context, the security of a block cipher translates into the exponential decay of OTOCs as a function of “computational” time, a behavior which in quantum systems signals the approach to a chaotic state [6–12].

The principal conclusion of this paper is that one can build classical block ciphers on n bits, secure to polynomial attacks, with as few as $\mathcal{O}(n \log n)$ gates in circuits of depth $\mathcal{O}(\log n)$. We believe that this result, as well as the physics-inspired approach proposed in this paper, should have important implications to many cryptographic applications, especially those requiring fast rates of encryption when dealing with large data sets. More importantly, shallow ciphers of this type are the basis for a proposed Encrypted-Operator Computing (EOC) scheme that allows one to carry out computations directly on encrypted data via encrypted operators (or circuits), an alternative to Homomorphic Encryption [13] presented in Ref. [14].

The important conceptual element of this paper is to map strings of Pauli operators describing classical attacks into a dual quantum mechanical space of strings in which the evolution of string operators is translated into evolution in a Hilbert space of strings. Within this string picture, the computation implemented by universal classical gates evolves an initial string into a *superposition* of string states. The special feature which makes the quantum mechanical analogy non-trivial is the presence of nonlinear classical gates g in bit space [i.e., those for

which $g(x \oplus y) \neq g(x) \oplus g(y) \oplus c$, for constant c]. It is this nonlinearity that leads to the proliferation of string components making up the quantum superposition, by contrast with linear gates, which can only change the state of a single string. Thus, as a result of evolution via nonlinear gates, the string wave function spreads over the full Hilbert space of strings, reaching an asymptotic state that cannot be distinguished from a random wave function drawn from an ensemble that respects all the symmetries of the system. It is the closeness to this asymptotic state that measures the quality of the classical cipher, and it is the evolution towards this state that defines the speed of the scrambling process.

Here we quantify the delocalization of the wave function in string space in terms of generalized inverse participation ratios [15], and corresponding entropies. In the asymptotic state, these entropies reach their maximum values, which include a universal correction of order 1 that only depends on the symmetries of the wave functions, as we illustrate through a comparison between classical circuits built from 3-bit permutation gates in S_8 and quantum circuits of 2-qubit gates in either $U(4)$ or $O(4)$. The discrete or continuous, real or complex nature of the wave function in string space is preserved under evolution, defining three distinct symmetry classes: permutation, orthogonal, and unitary. Moreover, the asymptotic-state OTOCs vanish, which together with the maximum entropy reflect the chaotic and irreversible nature of the evolution.

We view the residual entropy – the difference from the maximum entropy – as the measure of how much information can be extracted by an adversary. We illustrate this principle by computing the entropies for a Feistel cipher as function of the number of rounds. We show that: (a) for 1 or 2 rounds the entropy differs by an extensive amount from the maximum; (b) for 4 or more rounds the entropy reaches its maximum up to exponentially-small finite-size corrections; and (c) for 3 rounds the entropy reaches its extensive maximum but with an order 1 deficit with respect to the universal (order 1) correction. These results are consistent with the conclusions of the classic Luby-Rackoff work [2], and reflect the fact that a Feistel cipher with 4 or more rounds yields a strong-pseudorandom permutation, while a 3-round cipher is “marginal” in that a combined 3-query plaintext/ciphertext attack (that exploits the regular structure of the alternating left/right rounds of the Feistel cipher) can distinguish the resulting permutation from a strong-pseudorandom one [16].

Arguably, the main contribution of this paper is to determine, for a cipher built via random reversible classical circuits, the minimum number of 3-bit gates needed to reach the asymptotic random multi-string wave function. Physically, the evolution to this asymptotic state occurs through quantum diffusion in string space, controlled by transition amplitudes between string states induced by the action of gates in bit space. We study the statistics of these transition amplitudes and their associated

transition probabilities for the case of interest, the 3-bit permutation gates, and compare it to the cases of 2-qubit quantum orthogonal and unitary gates. As shown explicitly in this paper, the essential feature in all three symmetry classes is that the evolution via universal gates leads to string proliferation due to non-zero matrix elements between an initial string state and multiple final states.

As already mentioned above, we find that the minimum size circuit leading to the vanishing of the OTOCs to exponential precision and the saturation of the entropy scales as $\mathcal{O}(n \log n)$. In the context of the cipher, this implies that the action of a random circuit of this size cannot be distinguished from a pseudorandom permutation with a polynomial number of queries. Establishing this result requires eliminating a bottleneck associated with the probability that small initial strings do not grow sufficiently fast. This bottleneck occurs because the evolution through generic gates results in a non-zero stay-probability, p , for size (or weight) 1 substrings; which, in turn, translates into a tail in the distribution of string sizes that scales as p^ℓ after the application of ℓ layers of $n/3$ non-overlapping 3-bit gates. These tails lead to an undesirable polynomial in n decay of the OTOCs for $\ell \sim \log n$. We eliminate these tails by structuring the circuit so as to separate two distinct processes: (a) the extension of a small weight string in the initial state to a string of macroscopic weight; and (b) the splitting of the resulting macroscopic string into a superposition of exponentially many string states, a process necessary for the decay of the residual entropy and the OTOCs. We identify specific subsets of gates of S_8 that separately implement these processes, which we refer to as “inflation” and “proliferation”, respectively. Inflation is implemented via circuits built by drawing from a set of 144 special linear gates (out of the $8!$ 3-bit permutation gates) for which the stay-probability for weight 1 substrings vanishes. In bit space, these gates flip two or more bits at the output when a single bit is flipped at the input. String proliferation is implemented using a subset of S_8 with 10752 “super-nonlinear” 3-bit gates that maximize entropy production.

We use the special features of these gate sets to build a three-stage cipher, with a circuit of super-nonlinear gates bookended by two circuits of inflationary gates. Each of these circuits is structured in layers of 3-bit gates that cover all n bitlines (we assume for simplicity that $n = 3^q$, for an integer q). The wiring of the circuit – the choice of triplets of bits that are acted upon by 3-bit gates in each and every layer – follows a hierarchical (tree) structure. This choice allows us to carry out our calculations analytically, and most importantly, it accelerates scrambling as it mimics a system in infinite spatial dimensions. We show that this three-stage cipher, with $\mathcal{O}(\log n)$ layers of gates in each stage, leads to the exponential vanishing of OTOCs and the saturation of the entropy to the value associated with a random permutation. We thus claim that the action of our three-stage cipher of $\mathcal{O}(n \log n)$ gates cannot be distinguished from a random permuta-

tion with a polynomial number of queries.

We should stress that the mapping to string space highlights a connection between classical ciphers and the problem of scrambling by random quantum circuits [17–22]. This problem has engendered a great deal of interest in the context of the recent demonstration of quantum supremacy [23], as well as in studies of information processing in black holes, which are conjectured to be the fastest scramblers in nature [8–10, 12, 24, 25]. In the case of random quantum circuits, resolving the bottleneck associated with the growth of small strings that we mentioned above, requires circuits of sizes $\mathcal{O}(n \log^2 n)$ [19, 20, 22]. Our work suggests that, as in the classical cipher, one can further reduce the circuit size to $\mathcal{O}(n \log n)$ gates in the quantum case by deploying the three-stage construction described here. It remains to be determined whether the inflationary period can be implemented via the unstructured (i.e., random) placement of 2-qubit gates or it requires using our 144 linear 3-bit gates or their circuit-equivalent built from the correlated placement of 2-qubit CNOT gates.

Finally, we expect that ciphers based on random circuits are immune to quantum attacks. Known vulnerabilities to such attacks arise as a result of periodicities induced by design regularities, such as the right/left structure of rounds in Feistel ciphers [26], regularities that are absent in both classical and quantum random circuits.

The plan of the paper is as follows: in Sec. II we introduce notation and formulate classical ciphers and general attacks in terms of OTOCs, the vanishing of which establish a criterium for cipher security. With the notation and formal framework in place, we are in position to summarize our key conceptual contributions in Sec. III, setting up the roadmap for the rest of the paper. In Sec. IV we formulate the dynamics of the Pauli operators entering the OTOCs as a quantum evolution problem in a dual string space. In this subsection we also introduce generalized inverse participation ratios and their associated entropies for quantifying the delocalization of the wave function in string space. In Sec. V we derive the equilibrium distribution for the string wave function amplitudes for random permutations, and compare with those obtained for random unitary and orthogonal transformations, and extract bounds on the entropies for all three symmetry classes (see subsection VC). Subsection VB focuses on the case of permutations and uses entropies as diagnostics for the security of Feistel ciphers, providing a direct connection to the well-known results of Luby and Rackoff [2]. In subsection VD we establish the vanishing of OTOC in the equilibrium state characterized by independently and identically distributed string amplitudes, $A_{\beta\alpha}$. We turn to the dynamics of the approach to the asymptotic equilibrium state in Sec. VI, where we emphasize the common origin of string spreading in the structure of the string-space transition matrix elements for the three symmetry classes of gates, and argue for the same universal scaling of the minimum size circuit and the equilibration times for classical and quantum

circuits. In the same section we discuss the subtlety connected with long tails in the distribution of string weights that slow down scrambling by both classical and quantum random circuits. In subsections VIA and VIB we single out two distinct processes - string “inflation” and string “proliferation” - and the respective sets of gates in S_8 that implement them: linear “inflationary” gates which grow/inflate single strings and eliminate the above mentioned long tails in the distribution of string weights, and super-nonlinear gates which accelerate the proliferation in the number of strings, and are responsible for the saturation of string entropies. These two sets of gates are deployed in Sec. VII in the construction of a three-stage cipher - a central element of this work. In subsection VIIA we introduce a tree-structured wiring of the three-stage cipher circuit that accelerates scrambling, and also allows us to establish the main results of the paper analytically. Some important properties of the inflationary and proliferation stages of the tree-structured cipher are discussed in subsections VII B and VII C, respectively. These are then brought together in subsection VII D, where we present recursion relations for the Strict Avalanche Criterium (SAC) OTOC for arbitrary numbers of layers of gates, for each of the three stages of the cipher circuit. The subsection illustrates the behavior of these recursion relations, explains the mechanism for the exponential decay of the SAC OTOC with n , and documents the agreement with direct numerical simulations of the OTOC. Taken together, the results of Sec. VII confirm that the tree-structured three-stage circuits provide an implementation of classical ciphers secure to polynomial attacks with as few as $\mathcal{O}(n \ln n)$ gates. The paper ends in Sec. VIII with concluding remarks and questions for future research.

II. BLOCK CIPHERS AND REVERSIBLE COMPUTATION

A block cipher is a permutation, P , that acts on the space of binary states of n bits, i.e., P is an element of the symmetric group S_{2^n} . Permutations can be thought of as reversible classical computations, which can be encoded in circuits of universal reversible gates acting on a small number of bits. More precisely, even permutations can be decomposed into products of small permutations (elements of S_8) acting on 3 bits at a time, as shown by Coppersmith and Grossman [3]. (The realization of odd permutations requires either one additional n -bit gate or one ancilla bit.) These small permutations can be represented using a set of universal reversible gates, for example NOT, CNOT, and Toffoli gates [27]; here we work directly with the small permutation gates in S_8 .

A. Notation

Hereafter we use quantum bracket notation, and represent a permutation P acting on a binary string $x \in \{0, 1\}^n$ as an operator \widehat{P} acting on a state $|x\rangle \equiv |x_0 x_1 \dots x_{n-1}\rangle$,

$$\widehat{P} |x\rangle = |P(x)\rangle. \quad (1)$$

The permutation operator \widehat{P} is unitary and real: $\widehat{P}^{-1} = \widehat{P}^\dagger = \widehat{P}^\top$.

In this representation, reading and flipping bits are implemented using the Pauli operators $\hat{\sigma}_i^z$ and $\hat{\sigma}_i^x$, respectively:

$$\begin{aligned} \hat{\sigma}_i^z |x\rangle &= (-1)^{x_i} |x\rangle \\ \hat{\sigma}_i^x |x\rangle &= |x_0 x_1 \dots \bar{x}_i \dots x_{n-1}\rangle, \end{aligned} \quad (2)$$

where \bar{x}_i is the negation of x_i . We also introduce $P_i(x)$ to denote the i -th bit of $P(x)$, which can be read via

$$\widehat{P}^\top \hat{\sigma}_i^z \widehat{P} |x\rangle = (-1)^{P_i(x)} |x\rangle. \quad (3)$$

Since the operator \widehat{P} evolves the input state $|x\rangle$ into the output state $|P(x)\rangle$, it is natural to interpret

$$\hat{\sigma}_i^z(\tau) \equiv \widehat{P}^\top \hat{\sigma}_i^z \widehat{P} \quad (4)$$

as the Heisenberg evolution of the operator $\hat{\sigma}_i^z$ in the course of the computation. Here τ defines the accumulated ‘‘time’’ of the computation, which counts the number of gates (or layers of gates as appropriate) of the circuit implementing the permutation P . More generally, we define $\widehat{O}(\tau) \equiv \widehat{P}^\top \widehat{O} \widehat{P}$ as well as $\widehat{O}(0) \equiv \widehat{O}$ which represent operators at the output and input ends of the cipher, respectively.

B. Cryptoanalysis via correlation functions

In the context of the quantum language defined above, a criterium for ‘‘good’’ ciphers will be expressed through the behavior of a class of correlation functions known as out-of-time-order correlators (OTOCs) [6–12]. Following cryptoanalysis, we diagnose the quality of the ciphers in terms of plaintext and ciphertext attacks corresponding

to arbitrary readouts and flips on both inputs and outputs.

Consider first a simple example of plaintext attack in which an adversary probes the sensitivity of the output bit j to flipping an input bit i , as expressed by

$$C_{\text{SAC}}^{ij} = \frac{1}{2^n} \sum_x (-1)^{P_j(x \oplus c_i) \oplus P_j(x)}, \quad (5)$$

with $c_i = 2^i$ and the bitwise XOR operation for two n -bit strings $x \oplus c_i$ implementing the flip of the i -th bit of x . The Strict Avalanche Criterium (SAC) test [28–30] requires the function $P_j(x \oplus c_i) \oplus P_j(x)$ to be balanced, i.e., to be 0 or 1 with equal frequency, and thus C_{SAC} to vanish. For random permutations, C_{SAC} vanishes up to corrections that are exponentially small in n . Notice that Eq. (5) requires summing over all 2^n initial states x ; in a practical attack, only a number of samples M (polynomial in n) is accessible, in which case an adversary cannot resolve C_{SAC} below a noise level of $\mathcal{O}(1/\sqrt{M})$.

Within the quantum notation, Eq. (5) can be cast as a correlation function,

$$\begin{aligned} C_{\text{SAC}}^{ij} &= \frac{1}{2^n} \sum_x \langle x | \hat{\sigma}_i^x(0) \hat{\sigma}_j^z(\tau) \hat{\sigma}_i^x(0) \hat{\sigma}_j^z(\tau) | x \rangle \\ &\equiv \text{tr} [\rho_\infty \hat{\sigma}_i^x(0) \hat{\sigma}_j^z(\tau) \hat{\sigma}_i^x(0) \hat{\sigma}_j^z(\tau)] , \end{aligned} \quad (6)$$

where $\rho_\infty \equiv \mathbb{1}/2^n$ can be viewed as an infinite temperature density matrix. This correspondence is evidenced by following the sequence of operators from right-to-left in the first line of Eq. (6):

1. $\hat{\sigma}_j^z(\tau)$ measures the value of the j -th bit, $(-1)^{P_j(x)}$, at the output and returns the system to the initial input state, $|x\rangle$;
2. $\hat{\sigma}_i^x(0)$ flips the i -th bit of the initial input state, $|x\rangle$, into $|x \oplus c_i\rangle$;
3. $\hat{\sigma}_j^z(\tau)$ measures the j -th bit, $(-1)^{P_j(x \oplus c_i)}$, at the output and returns the system to the input state $|x \oplus c_i\rangle$; and finally,
4. $\hat{\sigma}_i^x(0)$ flips the i -th bit back, returning the system to the initial state $|x\rangle$.

As a second more complex example, we consider an attack that distinguishes a Feistel cipher build via a 3-round Luby-Rackoff construction from a strong pseudorandom permutation. This cipher is vulnerable to a classical adaptive chosen plaintext and chosen ciphertext attack (CPCA) [16], involving three queries, which we translate into the following OTOC:

$$\begin{aligned} C_{\text{CPCA}}^{ij} &= \text{tr} [\rho_\infty \hat{\sigma}_j^x(0) \hat{\sigma}_i^x(\tau) \hat{\sigma}_i^z(0) \hat{\sigma}_i^x(\tau) \hat{\sigma}_j^z(\tau) \hat{\sigma}_j^x(0) \hat{\sigma}_j^z(\tau) \hat{\sigma}_i^z(0)] \\ &= (-1)^{\delta_{ij}} \text{tr} \left[\rho_\infty (\hat{\sigma}_i^z(0) \hat{\sigma}_i^x(\tau))^2 (\hat{\sigma}_j^z(\tau) \hat{\sigma}_j^x(0))^2 \right]. \end{aligned} \quad (7)$$

We note that the 4-round version of this cipher is immune to this attack, as are ciphers based on sufficiently long random reversible circuits.

III. SUMMARY OF CONCEPTUAL CONTRIBUTIONS

Having introduced the formal framework, we are in position to outline the four conceptual contributions of this paper. The first one is to represent any plaintext/ciphertext attack involving multiple readouts and/or flips of bits at both inputs and outputs in the form of an OTOC of Pauli string operators

$$\widehat{\mathcal{S}}_\alpha = \prod_{j \in \alpha^x} \hat{\sigma}_j^x \prod_{k \in \alpha^z} \hat{\sigma}_k^z, \quad (8)$$

namely

$$C_{\text{CPCA}}^{\alpha_1, \beta_1 \dots \alpha_k, \beta_k} = \text{tr} \left[\rho_\infty \widehat{\mathcal{S}}_{\alpha_1}(0) \widehat{\mathcal{S}}_{\beta_1}(\tau) \widehat{\mathcal{S}}_{\alpha_2}(0) \widehat{\mathcal{S}}_{\beta_2}(\tau) \dots \widehat{\mathcal{S}}_{\alpha_k}(0) \widehat{\mathcal{S}}_{\beta_k}(\tau) \right]. \quad (9)$$

A Pauli string is labeled by the set $\alpha = (\alpha^x, \alpha^z)$ of bit indices present in the string. (We choose to place all the $\hat{\sigma}^x$ operators to the left of the $\hat{\sigma}^z$ s¹.)

The second conceptual contribution is to tie the security of the cipher to the vanishing of OTOCs representing plaintext/ciphertext attacks. In the quantum case, for both Hamiltonian systems and evolution via random quantum circuits, the vanishing of OTOCs is associated with irreversibility and chaos [7–12].

The third contribution is to connect the vanishing of OTOCs to the delocalization of the dual string-space wave function via the growth in size and exponential proliferation in number of Pauli strings in the course of the computation. We quantify this delocalization in terms of generalized inverse participation ratios [15] and corresponding entropies, which saturate for a random string wave function, thus tying together the vanishing of the OTOCs and the vanishing of the residual entropies for random permutations.

Finally, the fourth contribution is to realize that one must break the circuit into three stages, separating the string-space “inflationary” and “proliferation” action of special collections of gates in S_8 . It is this three-stage structure that allows us to construct a cipher with as few as $\mathcal{O}(n \log n)$ gates for which OTOCs vanish to exponential precision, and the string entropies saturate.

IV. QUANTUM EVOLUTION IN STRING SPACE

The description of OTOCs in terms of strings in Eq. (9) brings out the connection to quantum mechanics that is critical to our analysis: time evolution leads to superpositions in string space. It is this correspondence that

allows us to unify results in classical and quantum random circuits.

We further note that while classical permutations are the principal motivation for this work, below we use \widehat{P} to denote a general unitary transformation, since in considering the connection to quantum computation \widehat{P} will be replaced by a unitary \widehat{U} or orthogonal \widehat{O} transformation. The special properties of permutation operators will be noted as needed.

The connection to quantum mechanics is made manifest by translating the string operators $\widehat{\mathcal{S}}_\beta$ and $\widehat{\mathcal{S}}_\alpha^\dagger$ defined by Eq. (8) into bra $\langle \beta |$ and ket $|\alpha\rangle$ states in a dual string space that inherits the inner product

$$\langle \beta | \alpha \rangle = \frac{1}{2^n} \text{tr} \left(\widehat{\mathcal{S}}_\beta \widehat{\mathcal{S}}_\alpha^\dagger \right) = \delta_{\beta\alpha}. \quad (10)$$

The states resulting from this operator-to-state correspondence should be viewed as tensor products of n qudits that label 4 possible Pauli operators at each position in the string. The Heisenberg evolution of the string operators

$$\widehat{\mathcal{S}}_\beta(\tau) \equiv \widehat{P}^\dagger(\tau) \widehat{\mathcal{S}}_\beta \widehat{P}(\tau) = \sum_\alpha A_{\beta\alpha}(\tau) \widehat{\mathcal{S}}_\alpha \quad (11)$$

corresponds to the evolution in Hilbert space of string states via the unitary operator \widehat{U}_P , namely,

$$\langle \beta(\tau) | = \langle \beta | \widehat{U}_P = \sum_\alpha A_{\beta\alpha}(\tau) \langle \alpha |, \quad (12)$$

where the transition amplitudes between string states α and β are given by

$$\begin{aligned} A_{\beta\alpha}(\tau) &= \langle \beta | \widehat{U}_P | \alpha \rangle \\ &= \frac{1}{2^n} \text{tr} \left(\widehat{P}^\dagger \widehat{\mathcal{S}}_\beta \widehat{P} \widehat{\mathcal{S}}_\alpha^\dagger \right). \end{aligned} \quad (13)$$

We note that if one breaks the operators \widehat{P} and \widehat{P}^\dagger above into gates, these appear sequentially bookending the operator $\widehat{\mathcal{S}}_\beta$ in reverse-time order or, using the cyclic property of the trace, the operator $\widehat{\mathcal{S}}_\alpha^\dagger$ in the natural time order. Thus, the amplitudes $A_{\beta\alpha}(\tau)$ can be viewed as

¹ By adding a phase $i^{\alpha^x \cdot \alpha^z}$ to $\widehat{\mathcal{S}}_\alpha$ – picking up an i each time both a $\hat{\sigma}_j^x$ and $\hat{\sigma}_j^z$ appear at the same j , or basically deploying the $\hat{\sigma}^y$ s as well – would make the string operator Hermitian. Here we prefer the definition Eq. (8) for the applications we consider, and work explicitly with both $\widehat{\mathcal{S}}_\alpha$ and $\widehat{\mathcal{S}}_\alpha^\dagger$ when needed.

describing either forward propagation from α to β or backward propagation from β to α . Moreover $A_{\beta\alpha}(\tau)$ satisfies the normalization conditions

$$\sum_{\beta} |A_{\beta\alpha}(\tau)|^2 = \sum_{\alpha} |A_{\beta\alpha}(\tau)|^2 = 1, \quad (14)$$

which follow from the unitarity of $\widehat{\mathcal{U}}_P$, itself a conse-

quence of preservation of the norm under time evolution:

$$\begin{aligned} \langle \beta | \widehat{\mathcal{U}}_P \widehat{\mathcal{U}}_P^\dagger | \alpha \rangle &= \langle \beta(\tau) | \alpha(\tau) \rangle \\ &= \frac{1}{2^n} \text{tr} \left(\widehat{P}^\dagger \widehat{S}_\beta \widehat{P} \widehat{P}^\dagger \widehat{S}_\alpha^\dagger \widehat{P} \right) \\ &= \langle \beta | \alpha \rangle. \end{aligned} \quad (15)$$

Using the string amplitudes $A_{\alpha\beta}$ we can re-express the OTOC in Eq. (9):

$$\begin{aligned} C_{\text{CPCA}}^{\alpha_1, \beta_1 \dots \alpha_k, \beta_k} &= \sum_{\gamma_1, \dots, \gamma_k} A_{\beta_1 \gamma_1}(\tau) A_{\beta_2 \gamma_2}(\tau) \dots A_{\beta_k \gamma_k}(\tau) \text{tr} \left[\rho_\infty \widehat{S}_{\alpha_1} \widehat{S}_{\gamma_1} \widehat{S}_{\alpha_2} \widehat{S}_{\gamma_2} \dots \widehat{S}_{\alpha_k} \widehat{S}_{\gamma_k} \right] \\ &= \sum_{\gamma_1, \dots, \gamma_k} A_{\beta_1 \gamma_1}(\tau) A_{\beta_2 \gamma_2}(\tau) \dots A_{\beta_k \gamma_k}(\tau) (-1)^{\sum_{i \leq j} \alpha_i^x \cdot \gamma_j^x} (-1)^{\sum_{i < j} \gamma_i^z \cdot \alpha_j^z} (-1)^{\sum_{i < j} \alpha_i^z \cdot \alpha_j^z} (-1)^{\sum_{i < j} \gamma_i^z \cdot \gamma_j^z} \\ &\quad \times \delta_{\alpha_1^x \oplus \dots \oplus \alpha_k^x, \gamma_1^x \oplus \dots \oplus \gamma_k^x} \delta_{\alpha_1^z \oplus \dots \oplus \alpha_k^z, \gamma_1^z \oplus \dots \oplus \gamma_k^z}. \end{aligned} \quad (16)$$

where the dot product is defined as $a \cdot b \equiv a_1 b_1 + \dots + a_n b_n$. An important quantity that will be used throughout the paper is the string weight, defined as $w(\alpha) \equiv \sum_i (\alpha_i^x \vee \alpha_i^z)$, which measures the number of non-identity Pauli operators that compose the string. (Each $\alpha_i^x \vee \alpha_i^z$ is 1 if at location i the string has an $\hat{\sigma}_i^x$, an $\hat{\sigma}_i^z$, or both operators, and is 0 otherwise.)

Note that the string operators in Eq. (8) were conveniently defined as product of real operators, using $\hat{\sigma}^x$ and $\hat{\sigma}^z$ s, to avoid factors of i when making the connection with the cipher attacks. The effect of $\hat{\sigma}^y$ s appears when $\hat{\sigma}^x$ and $\hat{\sigma}^z$ operators overlap in the string \widehat{S}_α ; we count the number of such overlaps by $n_y(\alpha) \equiv \alpha^x \cdot \alpha^z$. These strings are not self-conjugate and satisfy

$$\widehat{S}_\alpha^\dagger = (-1)^{\alpha^x \cdot \alpha^z} \widehat{S}_\alpha, \quad (17)$$

which, in turn, leads to the following symmetry relation, preserved throughout the evolution:

$$A_{\beta\alpha}^*(\tau) = (-1)^{\beta^x \cdot \beta^z} (-1)^{\alpha^x \cdot \alpha^z} A_{\beta\alpha}(\tau). \quad (18)$$

For permutations, the amplitudes are real, and this symmetry implies that $A_{\beta\alpha}(\tau)$ is non-zero if and only if $n_y(\alpha) = n_y(\beta) \bmod 2$. In terms of the permutations $P(x)$ on the bit strings x , the amplitudes take values in a discrete set, as can be seen from the explicit formula:

$$\begin{aligned} A_{\beta\alpha}(\tau) &= \frac{1}{2^n} \sum_x \langle x | \widehat{P}^\dagger \widehat{S}_\beta \widehat{P} \widehat{S}_\alpha^\dagger | x \rangle = \frac{1}{2^n} \sum_x \langle x | \widehat{P} \widehat{S}_\alpha^\dagger \widehat{P}^\dagger \widehat{S}_\beta | x \rangle \\ &= \frac{1}{2^n} \sum_x (-1)^{\alpha^z \cdot P^{-1}(x)} \langle P^{-1}(x) \oplus \alpha^x | P^{-1}(x \oplus \beta^x) \rangle (-1)^{\beta^z \cdot x} \\ &= \frac{1}{2^n} \sum_x (-1)^{\beta^z \cdot x} (-1)^{\alpha^z \cdot P^{-1}(x)} \delta_{\beta^x, x \oplus P(P^{-1}(x) \oplus \alpha^x)}. \end{aligned} \quad (19)$$

For orthogonal transformations, \widehat{O} , the amplitudes $A_{\beta\alpha}(\tau)$ are real but continuous, and Eq. (18) implies that $A_{\beta\alpha}(\tau)$ is non-zero if and only if $n_y(\alpha) = n_y(\beta) \bmod 2$, just as for permutations. For unitary transformations, \widehat{U} , the amplitudes are also continuous and Eq. (18) implies two cases according to the relative parity of $n_y(\alpha)$

and $n_y(\beta)$: (a) for $n_y(\alpha) = n_y(\beta) \bmod 2$, the amplitudes $A_{\beta\alpha}(\tau)$ are real; and (b) for $n_y(\alpha) \neq n_y(\beta) \bmod 2$, the amplitudes $A_{\beta\alpha}(\tau)$ are purely imaginary.

We note that our discussion also applies for backpropagation via the inverse operators (e.g., the inverse permutation P^{-1}) by exchanging \widehat{P} and \widehat{P}^\dagger through a “time-

reversal” transformation:

$$\begin{aligned} A_{\alpha\beta}(-\tau) &\equiv \langle \alpha | \widehat{U}_{P^{-1}} | \beta \rangle \\ &= \frac{1}{2^n} \text{tr} \left(\widehat{P} \widehat{S}_\alpha \widehat{P}^\dagger \widehat{S}_\beta^\dagger \right) \\ &= A_{\beta\alpha}^*(\tau). \end{aligned} \quad (20)$$

Given the operator-to-state correspondence defined above, the main results of the paper will follow from the behavior of the string amplitudes $A_{\beta\alpha}(\tau)$ as functions of τ . These wave function amplitudes will allow us to quantify (a) the delocalization in string space in analogy with measures of (de)localization in quantum systems, and (b) the time, τ_{scramble} , needed for the amplitudes to approach those of a maximally scrambled state. In particular, this random state is the equilibrium state with maximum entropy and vanishing OTOCs. The connection between attacks and OTOCs implies that the random classical circuit leads to a secure cipher after time τ_{scramble} .

For a fixed initial string state α , the amplitudes $A_{\beta\alpha}$ represent a wave function in a $d = 4^n$ dimensional Hilbert space. Delocalization in this space can be quantified via the generalized inverse participation ratios and their associated entropies that are defined, respectively, by

$$\mathcal{P}_q = \sum_{\beta} |A_{\beta\alpha}(\tau)|^{2q}, \quad (21)$$

and

$$S_q = \frac{1}{1-q} \ln \mathcal{P}_q. \quad (22)$$

These provide concrete and intuitive measures of information scrambling, reflected in the proliferation of strings and delocalization in string space. In particular: $\mathcal{P}_{q \rightarrow 0+}$ measures the number of non-zero amplitudes $A_{\beta\alpha}$, thus counting the number of strings,

$$\mathcal{N}_s = \mathcal{P}_{q \rightarrow 0+}; \quad (23)$$

$S_{q \rightarrow 1}$ gives the information entropy,

$$S = - \sum_{\beta} |A_{\beta\alpha}(\tau)|^2 \ln (|A_{\beta\alpha}(\tau)|^2); \quad (24)$$

and

$$\mathcal{P}_2 = \sum_{\beta} |A_{\beta\alpha}(\tau)|^4 \quad (25)$$

is the inverse participation ratio, familiar from the theory of localization in quantum systems [15].

V. EQUILIBRIUM

Before we focus on the dynamics of delocalization in string space and the approach to equilibrium, we discuss the asymptotic equilibrium state. At equilibrium,

the string wave functions $A_{\beta\alpha}$ become independently distributed over string space, i.e., over different initial and final states α and β . The independent distributions are however constrained by the normalization condition, Eq. (14), the parity condition, Eq. (18), as well as the symmetry class of the underlying transformation defining the computation. Below we derive the explicit probability distributions for the amplitudes $A_{\beta\alpha}$ for the three symmetry classes associated with permutations, orthogonal, and unitary transformations.

A. Random permutations

We start by considering the equilibrium statistical properties of the string amplitudes $A_{\beta\alpha}$ for truly random permutations, with no reference to how they are built. In particular, we compute the probability distribution for the string amplitudes $A_{\beta\alpha}$, from which we obtain the generalized inverse participation ratios and entropies characterizing the equilibrium state.

The form of the probability distributions of the $A_{\beta\alpha}$ amplitudes can be obtained explicitly in the large- d regime as follows. Starting from Eq. (19), notice that the values of β^x that collect non-zero contributions from the summation over binary states x must satisfy

$$\beta^x = x \oplus \tilde{P}(x), \quad (26)$$

where

$$\tilde{P}(x) \equiv P(P^{-1}(x) \oplus \alpha^x). \quad (27)$$

For any permutation P , the associated permutation \tilde{P} is an involution, i.e., $\tilde{P}^2 = \mathbb{1}$, for any α^x . Now notice that the pair of state values x and $\tilde{P}(x)$ contribute to the same β^x “box”, since $x \oplus \tilde{P}(x) = \tilde{P}(x) \oplus \tilde{P}(\tilde{P}(x)) = \tilde{P}(x) \oplus x$. We thus partition the set of $N = 2^n$ values of x into $N/2$ pairs $(x_1, x_2), \dots, (x_{N-1}, x_N)$, where $x_{2j} = \tilde{P}(x_{2j-1})$, $j = 1, \dots, N/2$. For a random P , the number of pairs that fall into a given β^x box (due to $x_{2j-1} \oplus x_{2j} = \beta^x$) should be Poisson distributed, i.e., the probability that m pairs fall into box β^x is

$$p_m = e^{-1/2} \frac{1}{m!} \frac{1}{2^m}, \quad (28)$$

where the Poisson parameter is $1/2$ (since there are $N/2$ pairs for N boxes).

Next, let us consider the phases, i.e., signs of contributions to Eq. (19). The phases coming from the two entries in a pair interfere either constructively if $\beta^x \cdot \beta^z = \alpha^x \cdot \alpha^z \pmod{2}$, or destructively if $\beta^x \cdot \beta^z \neq \alpha^x \cdot \alpha^z \pmod{2}$. The two cases can be considered together by defining $\eta \equiv \beta^x \cdot \beta^z + \alpha^x \cdot \alpha^z \pmod{2}$. More precisely, by using the identities $P^{-1}(\tilde{P}(x)) = P^{-1}(x) \oplus \alpha^x$ [see Eq. (27)] and $\tilde{P}(x) \oplus \beta^x = x$ [see Eq. (26)], we can relate the phases associated with the two partners, $\tilde{P}(x)$ and x , in a pair

as follows:

$$\begin{aligned}
& (-1)^{\beta^z \cdot \tilde{P}(x)} (-1)^{\alpha^z \cdot P^{-1}(\tilde{P}(x))} \\
&= (-1)^{\beta^z \cdot \tilde{P}(x)} (-1)^{\alpha^z \cdot P^{-1}(x)} (-1)^{\alpha^z \cdot \alpha^x} \\
&= (-1)^{\beta^z \cdot \tilde{P}(x)} (-1)^{\alpha^z \cdot P^{-1}(x)} (-1)^{\beta^z \cdot \beta^x} (-1)^\eta \\
&= (-1)^{\beta^z \cdot [\tilde{P}(x) \oplus \beta^x]} (-1)^{\alpha^z \cdot P^{-1}(x)} (-1)^\eta \\
&= (-1)^{\beta^z \cdot x} (-1)^{\alpha^z \cdot P^{-1}(x)} (-1)^\eta, \tag{29}
\end{aligned}$$

and thus, as claimed above, the two contributions come either with the same sign if η is even, or with opposite signs if η is odd.

The interference described above implies that only half of the values of β^z result in a non-zero amplitude, which is computed as follows. Members of each pair will add ± 1 in phase, and thus contribute either $+2$ or -2 to the amplitude. Let m_\pm denote the number of pairs falling within a β^x box contributing ± 2 , respectively. The probability that the amplitude $A = 2r/N$ is

$$\begin{aligned}
p(A = 2r/N) &= \sum_m e^{-1/2} \frac{1}{m!} \frac{1}{2^m} \sum_{m_+ + m_- = m} \frac{m!}{m_+! m_-!} \frac{1}{2^{m_+}} \frac{1}{2^{m_-}} \delta_{r, m_+ - m_-} \\
&= e^{-1/2} \sum_{m_+, m_-} \frac{1}{m_+!} \frac{1}{m_-!} \frac{1}{4^{m_+}} \frac{1}{4^{m_-}} \delta_{r, m_+ - m_-} \\
&= e^{-1/2} \sum_k \frac{1}{(|r| + k)!} \frac{1}{k!} \left(\frac{1}{4}\right)^{|r| + 2k} \\
&= \frac{1}{\sqrt{e}} I_{|r|}(1/2), \tag{30}
\end{aligned}$$

where $I_\nu(z)$ is the modified Bessel function.

To compute the moments, it is useful to introduce the generating function

$$\begin{aligned}
\tilde{p}(w) &= \sum_{r=-\infty}^{\infty} p(A = 2r/N) e^{iwr} \\
&= e^{-1/2} \sum_{m_+, m_-} \frac{1}{m_+!} \frac{1}{m_-!} \frac{1}{4^{m_+}} \frac{1}{4^{m_-}} e^{iw(m_+ - m_-)} \\
&= e^{-\frac{1}{2}} e^{\frac{1}{2} \cos w}. \tag{31}
\end{aligned}$$

The corresponding (averaged) generalized participation ratios are given by

$$\overline{\mathcal{P}}_q = d^{1-q} 2^{2q-1} \frac{1}{\sqrt{e}} \left(-i \frac{\partial}{\partial w} \right)^{2q} e^{\frac{1}{2} \cos w} \Big|_{w=0}. \tag{32}$$

The associated equilibrium entropies display an extensive (volume) contribution and a correction, ΔS_q^{eq} , of order 1:

$$S_q^{\text{eq}} = n \ln 4 - \Delta S_q^{\text{eq}}, \tag{33}$$

where

$$\Delta S_q^{\text{eq}} = \frac{1}{q-1} \ln \left[\frac{1}{2\sqrt{e}} \left(-2i \frac{\partial}{\partial w} \right)^{2q} e^{\frac{1}{2} \cos w} \Big|_{w=0} \right]. \tag{34}$$

(We note that in calculating the entropies we used annealed averages, since in the regime of delocalized string wave functions the quenched and annealed averages should coincide up to exponentially small corrections.)

For integer values, the ΔS_q^{eq} corrections can be read off from Eq. (34): for example $\Delta S_2^{\text{eq}} = \ln 10$, $\Delta S_3^{\text{eq}} = \frac{1}{2} \ln 196 = \ln 14$, and $\Delta S_4^{\text{eq}} = \frac{1}{3} \ln 6280$. The value $\Delta S_1^{\text{eq}} = 1.9618961$ is obtained numerically from the probabilities in Eq. (30). These residual entropies are used in the next sub-section to diagnose the quality of a Feistel cipher.

B. Application to Feistel ciphers

A Feistel cipher, also referred to as a Luby-Rackoff cipher [1, 2], builds a pseudorandom permutation by using pseudorandom functions. The construction of the cipher proceeds by first separating n bits (n even) into left (L) and right (R) registers with $n/2$ bits each. Denoting the input to the cipher by the pair (L_0, R_0) , one then iterates through rounds $k = 1, \dots, r$, according to:

$$\begin{aligned}
L_k &= R_{k-1} \\
R_k &= L_{k-1} \oplus f_k(R_{k-1}), \tag{35}
\end{aligned}$$

where f_k , $k = 1, \dots, r$, are different pseudorandom functions with $n/2$ -bit inputs and outputs. The it-

erations in Eq. (35) define a permutation P such that $(L_r, R_r) = P(L_0, R_0)$. The inverse permutation, $(L_0, R_0) = P^{-1}(L_r, R_r)$, is obtained by starting with (L_r, R_r) and working backwards, for $k = r, \dots, 1$, using the recursion

$$\begin{aligned} R_{k-1} &= L_k \\ L_{k-1} &= R_k \oplus f_k(L_k). \end{aligned} \quad (36)$$

Luby and Rackoff [2] proved that a 3-round (4-round) cipher is indistinguishable from a random permutation when interrogated with a polynomial number of one-sided or plaintext queries (two-sided or plaintext/ciphertext queries). [An example of a plaintext/ciphertext attack on a 3-round Feistel cipher was represented as an OTOC in Eq. (7).]

Below we apply our criterium for a secure cipher based on the saturation of the entropies to the Luby-Rackoff cipher. We compute the entropies defined in Eq. (22) us-

ing the string amplitudes $A_{\beta\alpha}$ in Eq. (19), calculated by using the permutations P, P^{-1} of the Feistel cipher for an initial string α that corresponds to a $\hat{\sigma}^x$ operator (or NOT gate) on a bit on the L register of the cipher. As shown in Fig. 1(a), we find that the entropy S_1 marches to its asymptotic equilibrium value S_1^{eq} [see Eq. (33)] as the number of rounds increases. Figure 1(b) displays the average (over different realizations of ciphers) residual entropy $S_1^{\text{eq}} - \bar{S}_1$, and shows that the extensive contribution is saturated for 3 or more rounds, as reflected in the crossing of the curves for different block sizes at exactly 3 rounds. However, the saturation of the remaining order 1 contribution to the asymptotic equilibrium value, $\Delta S_1^{\text{eq}} = 1.9618961$, computed in the previous subsection requires at least 4 rounds. The same saturation behavior is illustrated in Table I for other entropies ($q \neq 1$). It is important to note that at 4 (or more) rounds $\Delta S_1^{\text{eq}} - \overline{\Delta S}_1$ vanishes exponentially in the number of bits, n , as seen in the inset to Fig. 1(b).

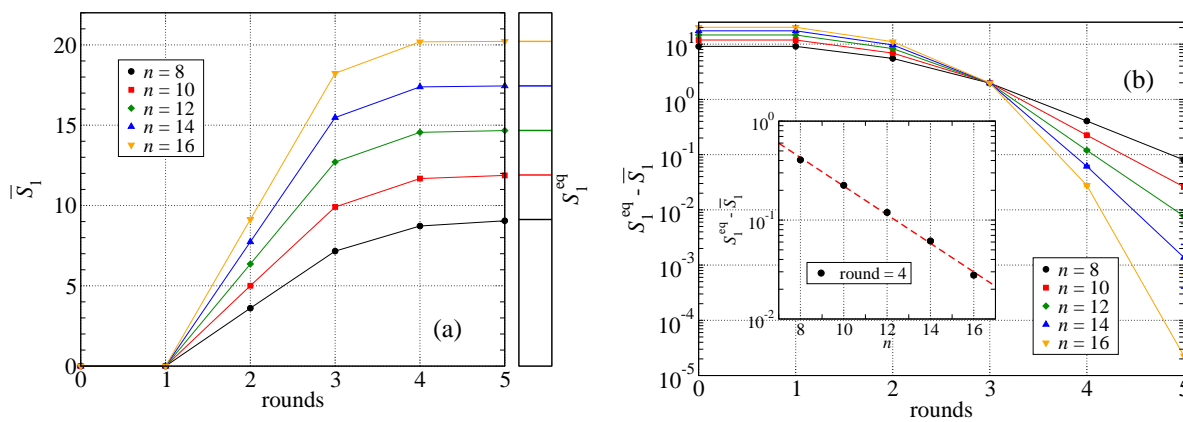


FIG. 1. (a) Average entropy, \bar{S}_1 , over different realizations of Feistel ciphers, as a function of the number of rounds, for different block sizes, n . The initial string contains a single $\hat{\sigma}^x$ on the L register ($\alpha^z = 0$ and $\alpha^x = 2^{n/2-1}$). The number of Feistel ciphers used in the averaging range from 500 ($n = 8$) to 100 ($n = 16$). Solid lines on the left panel are guides to the eye. The solid lines on the right sidebar panel show the equilibrium entropy values. (b) The deviation of entropy in panel (a) from the equilibrium value S_1^{eq} . Notice that the deviations increase (decrease) with n below (above) 3 rounds, whereas the deviation is independent of n after exactly 3 rounds. The inset in (b) shows the decrease in the deviation from the equilibrium entropy after 4 rounds as a function of the number of bits. The dashed line corresponds to the fitted function $S_1^{\text{eq}} - \bar{S}_1 = 6.2(9) e^{-0.33(1)n}$, where numbers in parentheses indicate standard errors. Pseudorandom functions used to build an n -bit cipher, f_k , $k = 1, \dots, r$, are obtained by r $n/2$ sequential calls to a pseudorandom bit function with equal probability for outputs 0 or 1.

The analysis of the entropy saturation gives an intuitive interpretation of the Luby and Rackoff results. Without knowledge of any specific attack, the order 1 residual entropy of 3-round ciphers underscores the vulnerability to an attack that can uncover of the order of 1 bit of information. At the same time, the exponential decay (with n) of the residual entropy of 4-round ci-

phers reflects the fact that such ciphers are secure against any polynomial attack. We note that while calculating the string entropy is exponentially costly, the finite size scaling analysis (common in statistical mechanics) establishes the above results by considering only computationally accessible sizes.

	round 1	round 2	round 3	round 4	round 5	rand. perm. (numerical)
$S_1^{\text{eq}} - \bar{S}_1$	22.1807	11.08(1)	1.98(1)	0.028(1)	0.00002(67)	0.00016(49)
$S_2^{\text{eq}} - \bar{S}_2$	22.1807	11.07(1)	2.7(1)	0.053(4)	0.0005(8)	0.00036(64)
$S_3^{\text{eq}} - \bar{S}_3$	22.1807	11.05(2)	4.1(3)	0.124(14)	0.0013(13)	0.00064(87)

TABLE I. Average residual entropies computed after rounds of a 16-bit Feistel cipher. Initial states and values of α^z and α^x are the same as those used in Fig. 1. 100 circuits are used to compute the average. Numbers in parentheses indicate standard deviations. The right-most column shows the residual entropy values for 16-bit random permutations computed numerically (average over 100 permutations). The values of $S_q^{\text{eq}} = 16 \ln 4 - \Delta S_q^{\text{eq}}$ for the q shown are computed from Eq. (33) with the corrections in Eq. (34), explicitly $\Delta S_1^{\text{eq}} = 1.9618961$, $\Delta S_2^{\text{eq}} = \ln 10$, and $\Delta S_3^{\text{eq}} = \ln 14$.

C. Orthogonal and Unitary transformations

The probability of the string amplitudes $A_{\beta\alpha}$ are much easier to compute for orthogonal and unitary transformations, which, unlike permutations, are continuous.

For the orthogonal case, the amplitudes are real and the distribution is Gaussian, with the width determined by the normalization condition in Eq. (14). The symmetry condition in Eq. (18) restricts the set of string labels α which lead to non-zero amplitudes to those satisfying the parity condition $n_y(\alpha) = n_y(\beta) \bmod 2$. This condition eliminates amplitudes on half of the string space, and thus the Gaussian distribution for the remaining $d/2$ states has width $\sqrt{2/d}$ (recall that $d = 4^n$):

$$p_O(A_{\beta\alpha}) = \sqrt{\frac{d}{4\pi}} e^{-\frac{d}{4} A_{\beta\alpha}^2}. \quad (37)$$

For the unitary case, the symmetry condition in Eq. (18) dictates that the amplitudes are real for $n_y(\alpha) = n_y(\beta)$ even, and purely imaginary for $n_y(\alpha) = n_y(\beta)$ odd. By contrast to the orthogonal case, the amplitudes are non-vanishing in all d states, and thus the width of the Gaussian distribution is $\sqrt{1/d}$:

$$p_U(A_{\beta\alpha}) = \sqrt{\frac{d}{2\pi}} e^{-\frac{d}{2} |A_{\beta\alpha}|^2}. \quad (38)$$

These probability distributions lead to the following order-1 corrections to the entropies:

$$\Delta S_q^O = \ln 4 + \frac{1}{q-1} \ln \frac{\Gamma(q + \frac{1}{2})}{\Gamma(\frac{3}{2})} \quad (39)$$

and

$$\Delta S_q^U = \ln 2 + \frac{1}{q-1} \ln \frac{\Gamma(q + \frac{1}{2})}{\Gamma(\frac{3}{2})}. \quad (40)$$

D. Vanishing of OTOCs at equilibrium

For all three symmetry classes, the OTOCs vanish in the equilibrium state. For independently and identically

distributed amplitudes $A_{\beta\alpha}$, the ensemble average of the expression in Eq. (16) factorizes into products of clusters of $2p$ As. In each of these clusters the states γ_i must be equal, and the cluster contributes a factor of A^{2p} . In all of the three symmetry classes discussed above, $A^{2p} \sim d^{-p}$.

When there are two or more clusters, the number of independent strings γ to be summed over is $\sum_p n_p - 1$, where n_p is the number of clusters of size $2p$, with the -1 reflecting the reduction in the number of independent γ s by 1 due to the Kronecker δ in Eq. (16). It then follows that the contribution to the OTOC from a given partition scales as $d^{-1 + \sum_p n_p - \sum_p n_p p}$; and thus, OTOCs are dominated by partitions with clusters of size 2 (or $p = 1$), the contribution of which vanishes as d^{-1} , the inverse of the size of the string Hilbert space. All other partitions contribute higher powers of d^{-1} . We note that the argument above did not take into account the phase factors coming from the traces over the products of string operators in Eq. (16); these factors, which introduce terms with alternating signs, can only further decrease the OTOCs.

In the case of a single cluster of size $2p$, there is only one γ to be summed over, and the Kronecker δ s in Eq. (16) simply specify the α s for which the correlator is non-zero. When $p \geq 2$, the contribution to the OTOC for one-cluster partitions, again not counting the phases (i.e., alternating signs) from the traces over the products of string operators in Eq. (16), vanishes as d^{1-p} , i.e., at least as fast as d^{-1} . By contrast, for the case of a single cluster with $p = 1$ one must consider the random phases, the sum over which, when weighted by the probabilities A^2 , leads to an additional factor of \sqrt{d} , and consequently, an OTOC decaying as $d^{-\frac{1}{2}}$.

These arguments are common to the three symmetry classes for generic string operators defining OTOCs. We note, however, that the case of permutations contains an invariant subspace of the Hilbert space of strings, namely the space of z -strings (these shall be further discussed in Sec. VI). An initial z -string, containing a product of only Pauli $\hat{\sigma}_z$ s and identities, will evolve into a superposition of z -strings. The SAC OTOC of Eq. (6) falls into this category in that the relevant string amplitudes, $A_{\beta\gamma}(\tau)$, spread initial z -strings only over a $\sqrt{d} = 2^n$ subspace (in-

stead of over the full 4^n -dimensional string space). Arguments exactly like those we made above for the single cluster with $p = 1$ still apply, but with the sum over the γ 's restricted to the subspace with $\gamma^x = 0$; this restriction implies that the OTOCs of this type will decay as $d^{-\frac{1}{4}}$.

As will become clear in the next section, reaching an equilibrium state of independently and identically distributed amplitudes $A_{\beta\alpha}$ that result in the vanishing of arbitrary order OTOCs, requires the use of a universal set of gates.

VI. STRING DYNAMICS

For permutations, the dynamics of the string amplitudes is determined by the specific implementation of P , for example, either through the rounds of a Feistel cipher or through the application of a universal set of classical gates. Here we focus on the evolution via a random classical circuit decomposed in terms of 3-bit gates in the symmetric group S_8 , each of which leads to a transition amplitude in string space of the form

$$\begin{aligned} t_{\alpha'\alpha}^{(g)} &= \langle \alpha' | \hat{g} | \alpha \rangle \\ &= \frac{1}{2^n} \text{tr} \left(\hat{g}^\dagger \hat{S}_{\alpha'} \hat{g} \hat{S}_\alpha^\dagger \right), \end{aligned} \quad (41)$$

where the string states α, α' may differ only in a substring of size 3. The transition amplitude $t_{\alpha'\alpha}^{(g)}$ implemented by a single gate g satisfies the same normalization conditions as the $A_{\beta\alpha}$, namely: $\sum_\alpha |t_{\alpha'\alpha}^{(g)}|^2 = \sum_{\alpha'} |t_{\alpha'\alpha}^{(g)}|^2 = 1$.

These matrix elements control the spreading of the string wave function in the $d = 4^n$ dimensional space of strings, analogous to the spreading taking place in random quantum circuits that deploy random unitary or orthogonal 2-qubit gates that are drawn from elements of $U(4)$ or $O(4)$, respectively. The essential feature that controls quantum diffusion and delocalization in string space is the connectivity of a given string state, α , to multiple states, α' , a feature which is common to all three gate-set symmetry classes mentioned above. Below we discuss these three classes of circuits – those using 3-bit gates in S_8 or 2-qubit gates in $U(4)$ or $O(4)$ – on equal footing.

To quantify spreading, we will consider powers of the transition probabilities $|t_{\alpha'\alpha}^{(g)}|^2$,

$$T_{\alpha'\alpha}^q = \frac{1}{|G|} \sum_{g \in G} |t_{\alpha'\alpha}^{(g)}|^{2q}, \quad (42)$$

averaged over the group G for the given gate set, and the sum over these quantities over all final states α' ,

$$V_\alpha^q = \sum_{\alpha'} T_{\alpha'\alpha}^q, \quad (43)$$

which are measures of the connectivity of the state α , averaged over gates. Notice that $V_\alpha^{q=1} = 1$ follows from the normalization condition $\sum_{\alpha'} |t_{\alpha'\alpha}^{(g)}|^2 = 1$, and thus in diagnosing string spreading we must consider V_α^q for $q \neq 1$. Since for a fixed initial state α the $|t_{\alpha'\alpha}^{(g)}|^2$ are probabilities, it is also useful to introduce an associated entropy

$$s_\alpha = -\frac{d}{dq} V_\alpha^q \Big|_{q \rightarrow 1} = -\sum_{\alpha'} \frac{1}{|G|} \sum_{g \in G} |t_{\alpha'\alpha}^{(g)}|^2 \ln |t_{\alpha'\alpha}^{(g)}|^2. \quad (44)$$

As the simplest example, consider 2-bit gates in S_4 or 2-qubit Clifford gates [31, 32], in which case $|t_{\alpha'\alpha}^{(g)}|^2$ is a permutation matrix, i.e., it connects single initial and final states, resulting in $V_\alpha^q = 1$ for all qs , and the vanishing of the entropy s_α . By contrast, for 3-bit gates in S_8 and 2-qubit unitary and orthogonal gates, $V_\alpha^q \neq 1$ for $q \neq 1$, and $s_\alpha > 0$. Table II displays the values of $V_\alpha^{q \rightarrow 0}$, which measures the average connectivity of a state α , and the entropy s_α . These results follow from the detailed structure of the matrix $T_{\alpha'\alpha}^q$ for 3-bit gates in S_8 , and 2-qubit gates in $U(4)$ and $O(4)$, shown in Fig. 2. For all three sets of gates and in all non-trivial subspaces, $V_\alpha^{q \rightarrow 0} > 1$ and $s_\alpha > 0$. It is then clear that string proliferation builds up exponentially through the application of a sufficiently large number of consecutive gates. It is this proliferation that evolves the entropies to their saturation values and leads to vanishing OTOCs in the asymptotic equilibrium state.

Measure	3-bit gates in S_8				2-qubit gates in $O(4)$			2-qubit gates in $U(4)$	
	Sector				Sector			Sector	
	identity	z-strings	odd parity	even parity	identity	odd parity	even parity	identity	other strings
$V_\alpha^{q \rightarrow 0}$	1	17/5	51/5	103/10	1	3	9	1	15
s_α	0	1.11	2.03	2.08	0	0.67	1.34	0	1.90

TABLE II. Connectivity and entropy measures for 3-bit permutation gates from S_8 ; and 2-bit gates in $O(4)$ and $U(4)$.

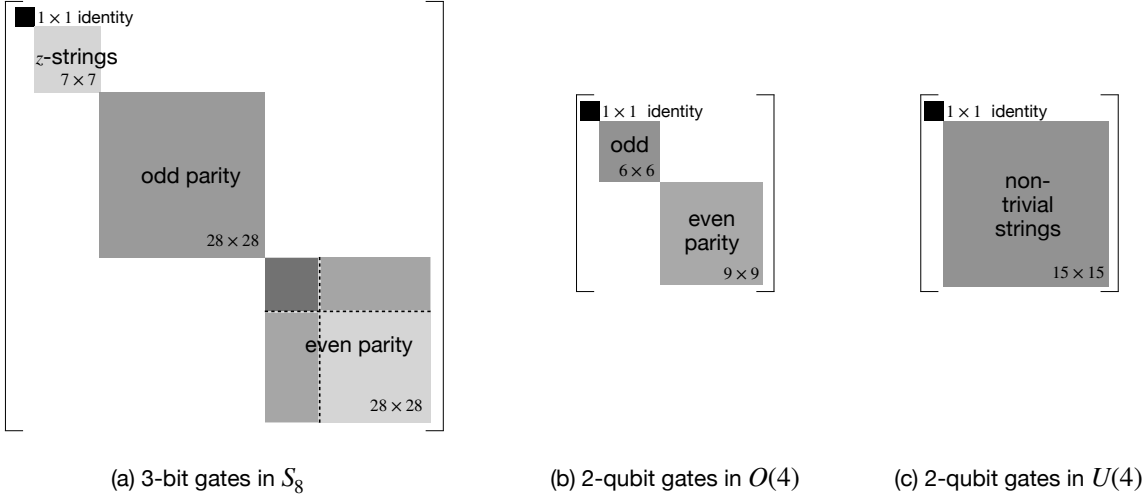


FIG. 2. Block form for the matrices $T_{\alpha'\alpha}^q$ in Eq. (42) for the three symmetry classes. (a) For 3-bit permutation gates, the $4^3 \times 4^3$ matrix T^q breaks up into 4 blocks of sizes 1×1 , 7×7 , 28×28 , and 28×28 , reflecting the symmetries of the string space transition amplitudes. The 1×1 block represents the transition between identity strings – tensor products of Pauli identity operators – that are invariant under evolution. The 7×7 block connects only z -string states, i.e., those with $\alpha_x = 0$, which form an invariant subspace. The remaining two 28×28 blocks correspond to transitions within subspaces with even or odd number $n_y(\alpha)$ of $\hat{\sigma}^y$ Pauli matrices or, equivalently, the number of overlapping $\hat{\sigma}^x$ and $\hat{\sigma}^z$ Pauli matrices on the substring. Recall from the discussion in connection with Eq. (18) that the parity of $n_y(\alpha)$ is a conserved quantity. The matrix elements of T^q within each of the 1×1 , 7×7 , and odd parity 28×28 blocks are equal. The even parity 28×28 block involves four sub-blocks: a diagonal 7×7 block describing transitions between x -strings ($\alpha_z = 0$); another diagonal 21×21 block of transitions between the remaining odd parity state; and two off-diagonal, 7×21 and 21×7 rectangular blocks connecting these two subspaces. Within each of these sub-blocks, the matrix elements are the same. (b) For 2-qubit gates in $O(4)$, the $4^2 \times 4^2$ matrix T^q breaks up into the trivial 1×1 block (connecting the identity strings), a 6×6 odd subsector, and a 9×9 even subsector. The matrix elements are all equal within each block. (c) For the 2-qubit gates in $U(4)$, T^q breaks into the identity block and a 15×15 block, with all equal matrix elements, connecting all other states.

A subtlety of the evolution governed by the application of gates drawn uniformly from the universal set S_8 is the non-zero probability p (independent of n) that a string of weight 1 does not increase even when touched by a (dual) gate. [The same situation occurs for gates in $O(4)$ and $U(4)$.] This “stay-probability” arises from the general structure of the $T_{\alpha'\alpha}^q$, and implies that after ℓ layers this probability decreases to $\sim p^\ell$, corresponding to a polynomial decay in n for $\ell \sim \ln n$. Below we will use the freedom afforded us in the context of ciphers to design circuits that deploy different subsets of gates in S_8 in separate stages. These multi-stage structure of circuits (of depth $\ell \sim \ln n$), which eliminate the tails due to low weight strings, rely on separating two distinct processes controlling the evolution of string wave function amplitudes: (a) the extension of the weight of the string, which we refer to as *inflation*; and (b) the proliferation of the number string states with non-zero amplitudes. The latter, but not the former, requires the action of non-linear gates. Below we discuss these distinct processes, *inflation* and *proliferation*, which will be central to the

structure of the optimal cipher proposed in this paper.

A. Inflation

The inflationary process is achieved through the action of a set of special gates that eliminate the stay-probability for weight 1 substrings. We handpick these special gates as follows. First, we compute the entries $t_{\alpha'\alpha}^{(g)}$ of the 64×64 transition in Eq. (41) for each of the $8!$ gates in S_8 . We then filter out all gates for which the 9×9 submatrix connecting the 9-dimensional subspace of weight 1 strings is non-zero, thus retaining only gates for which weight 1 substrings grow into weight 2 or 3 substrings. We identify 144 such “inflationary” gates, which are linear. These gates are listed explicitly in Appendix B, where we also represent them in terms of equivalent circuits of CNOTs.

To gain further insight into the effect of the 144 inflationary gates, we note that, in bit space, this set of gates has the following property: for any input state, flipping

one input bit flips at least 2 output bits. It follows that, after ℓ layers, flipping one of the n input bits of a circuit leads to a cascade of 2^ℓ flipped output bits, and thus $\ell = \log_2(n/2)$ layers suffice to change half of the output bits. The cipher proposed in Sec. VII employs a tree-structured circuit (see below) for which such a cascade occurs, thus eliminating tails in the stay probability of low-weight strings.

B. Proliferation

As already discussed in connection with Table II, the increase in entropy is connected with the proliferation of strings induced through the action of nonlinear gates in S_8 . In order to speed up entropy production, instead of deploying the full set of $8!$ gates in S_8 , we use the subset of nonlinear gates that maximizes string proliferation at each step. This set is identified from the entries $t_{\alpha'\alpha}^{(g)}$ for every gate g by selecting those for which the number of non-zero elements in each line or column is maximal. We find 10752 “super-nonlinear” gates satisfying this criterion. For all these gates the squares of the non-zero elements take the same values within each of the blocks shown in Fig. 2. In each line or column there are: 4 equal values of $1/4$ in the 7×7 z -block; and 16 equal values of $1/16$ in both the 28×28 even and odd blocks. This structure implies that each of these gates leads to string proliferation with each and every application. From the scattering matrix elements one also determines the values of $V_\alpha^{q \rightarrow 0}$ that measure the average connectivity of a state α and the entropy s_α , shown in Table III (notice that these values are – through the design choice above – larger than the averages for the gates in S_8 in Table II.) We established that this super-nonlinear subset of gates constitute a universal set for classical computation by determining that the order of the group generated by particular pairs of gates in this subset is $8!$ ²

Measure	Super-nonlinear subset of gates in S_8			
	identity	z-strings	odd parity	even parity
$V_\alpha^{q \rightarrow 0}$	1	4	16	16
s_α	0	$2 \ln 2$	$4 \ln 2$	$4 \ln 2$

TABLE III. Connectivity and entropy measures for super-nonlinear gates, a subset (with cardinality 10752) of the set of $8!$ gates in S_8 .

Particularly relevant to our discussion below is the action of super-nonlinear gates on typical macroscopic weight strings generated via inflation. In the evolution of such strings with large cross section, the action of every super-nonlinear gate leads to a superposition of strings and thus, every layer of $n/3$ super-nonlinear gates increases the number strings exponentially in n , resulting in a macroscopic increase in the string entropy. We note, however, that the exponential proliferation of strings already induced by the action of one layer of nonlinear gates is, by itself, not sufficient to ensure the equilibration of the system. As will be explained in Sec. VII in the context of multi-stage tree-structured circuits, in order to reach the asymptotic probability distribution of string amplitudes discussed in Sec. V, one requires a minimum number of layers of both inflationary and super-nonlinear gates. This number is determined by the accuracy to which one requires the vanishing of the OTOCs or the saturation of the entropies, criteria which determine the security of the cipher.

VII. MULTI-STAGE CIPHER

Below we will exploit the features of the special inflationary and super-nonlinear gates described above to introduce a three-stage fast-scrambling cipher, the structure of which is illustrated in Fig. 3.

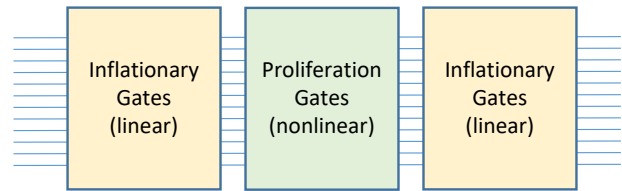


FIG. 3. A three-stage cipher, with two stages of inflationary gates flanking a stage of (super-)nonlinear gates.

More precisely, we break up the operator \hat{P} into three stages,

$$\hat{P} = \hat{L}_r \hat{N} \hat{L}_l \quad (45)$$

where the $\hat{L}_{l,r}$ are two different circuits composed of inflationary gates, placed to the left and right of a circuit \hat{N} of super-nonlinear gates, as depicted in Fig. 3. (The connectivity of these circuits are tree-structured as discussed below.) The general OTOC of Eq. (9) can be re-expressed as

² For example, the two permutations 01243675 and 73051246 suffice to generate S_8 .

$$C_{\text{CPCA}}^{\alpha_1, \beta_1 \dots \alpha_k, \beta_k} = \text{tr} \left[\rho_\infty \widehat{S}_{l(\alpha_1)}^N(0) \widehat{S}_{r(\beta_1)}^N(\tau) \widehat{S}_{l(\alpha_2)}^N(0) \widehat{S}_{r(\beta_2)}^N(\tau) \dots \widehat{S}_{l(\alpha_k)}^N(0) \widehat{S}_{r(\beta_k)}^N(\tau) \right], \quad (46)$$

where

$$\widehat{S}_{r(\beta)}^N(\tau) \equiv \widehat{N}^\dagger \widehat{S}_{r(\beta)} \widehat{N} \quad \text{and} \quad \widehat{S}_{l(\alpha)}^N(0) \equiv \widehat{S}_{l(\alpha)}, \quad (47)$$

with

$$\widehat{S}_{r(\beta)} \equiv \widehat{L}_r^\dagger \widehat{S}_\beta \widehat{L}_r \quad \text{and} \quad \widehat{S}_{l(\alpha)} \equiv \widehat{L}_l \widehat{S}_\alpha \widehat{L}_l^\dagger. \quad (48)$$

The inflationary (linear) circuits $\widehat{L}_{l,r}$ map single strings labeled by α and β onto single strings labeled by $l(\alpha)$ and $r(\beta)$, respectively. (We abuse notation and use l, r defining the specific inflationary circuits to also label the respective functions that map initial into final strings.)

The rewriting of the OTOC in Eq. (46) - in terms of products of large weight strings resulting from the inflation of the original initial and final state strings via layers of inflationary linear gates, which evolve through conjugation by the operator \widehat{N} , defined in Eq. (47) - provides an intuitive picture for the vanishing of OTOCs. The evolution of an inflated string from the output end with each layer of \widehat{N} yields an exponential number of strings, \mathcal{N}_s , that spread over the d -dimensional Hilbert space of strings. Following the arguments in Sec. VD, OTOCs are suppressed, at the very least, as the quartic root of \mathcal{N}_s , thus yielding OTOCs that vanish exponentially in n . This intuitive picture is borne out by an explicit calculation presented in Sec. VIID for the simplest SAC OTOC, using the tree-structured circuits of Sec. VII A. Moreover, this explicit calculation is consistent with the final conclusion of the paper (see below), namely, that $\mathcal{O}(\ln n)$ layers of gates, for each of the inflation and proliferation stages, are sufficient to suppress all OTOCs exponentially in n .

A. Tree-structured circuits

Below we describe in detail circuits mentioned in the introduction, in which triplets of bits acted upon by 3-bit gates are arranged in a hierarchical (tree) structure. We consider the case when n is a power of 3, $n = 3^q$. We proceed by forming groups of triplets of indices for each layer, selected as follows:

$$\begin{aligned} \ell = 1 : & \quad (0, 1, 2) (3, 4, 5) (6, 7, 8) \dots \\ \ell = 2 : & \quad (0, 3, 6) (1, 4, 7) (2, 5, 8) \dots \\ \ell = 3 : & \quad (0, 9, 18) (1, 10, 19) (2, 11, 20) \dots \\ \ell = 4 : & \quad (0, 27, 54) (1, 28, 55) (2, 29, 56) \dots \\ & \dots \end{aligned} \quad (49)$$

More precisely, each of the $n/3 = 3^{q-1}$ triplets in layer ℓ are indexed by (i, j, k) , which we write in base 3 as

$$\begin{aligned} i &= z_0 + 3 z_1 + 3^2 z_2 + \dots + 3^{\ell-1} \times \underline{0} + \dots + 3^{q-1} z_{q-1} \\ j &= z_0 + 3 z_1 + 3^2 z_2 + \dots + 3^{\ell-1} \times \underline{1} + \dots + 3^{q-1} z_{q-1} \\ k &= z_0 + 3 z_1 + 3^2 z_2 + \dots + 3^{\ell-1} \times \underline{2} + \dots + 3^{q-1} z_{q-1}, \end{aligned} \quad (50)$$

where $z_a = 0, 1, 2$, for $a = 0, \dots, q-1$. Notice that at layer ℓ the members of the triplets, (i, j, k) , are numbers that only differ in the $(\ell-1)$ -th trit, while the other $q-1$ trits z_a , $a \neq \ell-1$, enumerate the $3^{q-1} = n/3$ triplets. (If more than q layers are needed, we recycle in layer $\ell > q$ the triplets of layer $\ell \bmod q$.)

Once the triplets of indices, (i, j, k) , are selected for each layer, we map them onto groups of three bits indexed by, $(\pi(i), \pi(j), \pi(k))$, via a (randomly chosen) permutation π of the n bitlines. We note that for these tree-structure ciphers, the key consists of the data needed to specify the circuit, namely: (i) the permutation π ; and (ii) the list of gates in \mathcal{S}_8 chosen to act on each of the triplets, for all layers. This key uniquely defines the circuit, and its inverse.

B. String inflation with a tree-structured circuit

The tree-structured gate arrangement makes it rather simple to analyze the string inflation process. Let us consider the conjugation of the string operator \widehat{S}_α with the inflationary circuit \widehat{L}_l , $\widehat{S}_{l(\alpha)} \equiv \widehat{L}_l \widehat{S}_\alpha \widehat{L}_l^\dagger$. The conjugated string operator, $\widehat{S}_{l(\alpha)}$, can be written with the aid of Eq. (8) as

$$\begin{aligned} \widehat{S}_{l(\alpha)} &= \widehat{L}_l \left(\prod_{j \in \alpha^x} \hat{\sigma}_j^x \prod_{k \in \alpha^z} \hat{\sigma}_k^z \right) \widehat{L}_l^\dagger \\ &= \prod_{j \in \alpha^x} \left(\widehat{L}_l \hat{\sigma}_j^x \widehat{L}_l^\dagger \right) \prod_{k \in \alpha^z} \left(\widehat{L}_l \hat{\sigma}_k^z \widehat{L}_l^\dagger \right), \end{aligned} \quad (51)$$

whereby the inflation of the whole string is expressed in terms of the inflation of individual Pauli operators, on which we concentrate hereafter.

Each of the inflationary gates in a layer of \widehat{L}_l overlaps with a substring of length 3, and changes the weights of the substring upon conjugation, according to rates extracted from the transition matrices $t_{\alpha'\alpha}^{(g)}$ for gates g in the inflationary set. A weight 0 substring remains unchanged under conjugation. The conjugation of a single Pauli operator with the gate-operator \hat{g} generates a product of either 2 or 3 Pauli operators, i.e., the initial

weight 1 string expands to weight 2 or 3. (The expansion to weight 2 or 3 depends on the relative position of the initial Pauli operator with respect to the three bitlines on which the inflationary gate g acts; in 2 out of 3 cases it expands to weight 2, and in 1 out of 3 cases to weight 3.) There are also matrix elements for transitions of weight $2 \rightarrow 1$ (2 out of 3 cases) and $2 \rightarrow 2$ (1 out of 3 cases), as well as $3 \rightarrow 1$.

Using these transition rates, averaged over the gates in the inflationary set (which homogenizes effects of relative position between the Pauli operators on the string and the three bitlines), we carry out an analysis of the string growth within a mean-field treatment on the tree-structured circuit. Let us define the string density ρ of non-trivial Pauli operators as the weight w of a string divided by n . As a result of conjugation by a 3-bit inflationary gate, one obtains a recursion relation relating the string densities $\rho(\ell + 1)$ and $\rho(\ell)$ in consecutive layers:

$$\begin{aligned} \rho(\ell + 1) &= \frac{1}{3} \{ [1 - \rho(\ell)]^3 \times 0 \\ &\quad + \rho(\ell) [1 - \rho(\ell)]^2 [2 \times 2 + 3 \times 1] \\ &\quad + [\rho(\ell)]^2 [1 - \rho(\ell)] [1 \times 2 + 2 \times 1] \\ &\quad + [\rho(\ell)]^3 \times 1 \} \\ &= \frac{7}{3} \rho(\ell) - \frac{10}{3} [\rho(\ell)]^2 + \frac{4}{3} [\rho(\ell)]^3. \end{aligned} \quad (52)$$

In deriving this recursion we assume that the contributions to the weight of the substring due to each of the three bitlines acted upon by a gate are uncorrelated and uniform – for example, the probability that the substring has weight 3 is $[\rho(\ell)]^3$.

The recursion Eq. (52) has a fixed point at $\rho = 1/2$, which encodes that a single Pauli operator $\hat{\sigma}^x, \hat{\sigma}^y$ or $\hat{\sigma}^z$ on a given bitline would eventually evolve into a string of $\hat{\sigma}^x$ s, $\hat{\sigma}^y$ s, or $\hat{\sigma}^z$ s on half the bitlines. The approach to this asymptotic density is better captured by defining the quantity $m = 2\rho - 1$, and studying how fast it approaches 0. The recursion relation for m reads

$$m(\ell + 1) = \frac{2}{3} [m(\ell)]^2 + \frac{1}{3} [m(\ell)]^3. \quad (53)$$

We highlight the absence of a term linear in $m(\ell)$ on the right-hand side of Eq. (53), which makes the decay of m towards zero a double exponential in ℓ that, for $\ell \sim \mathcal{O}(\log n)$, translates into an exponential decay in n . Had we deployed the full set of gates in S_8 , the recursion relation would instead contain a linear in $m(\ell)$ term, slowing down the approach to the asymptotic value of the string density to exponential in ℓ and thus polynomial in n for similarly sized circuits, an issue connected to the stay-probabilities of string weights that we discussed above. (We return to the discussion of the presence of such linear terms in recursion relations derived for the SAC OTOC in Sec. VII D, where we also discuss the case of super-nonlinear gates.) Our analytical arguments lead to results in agreement with those obtained from numerical simulations, as shown in Fig. 4.

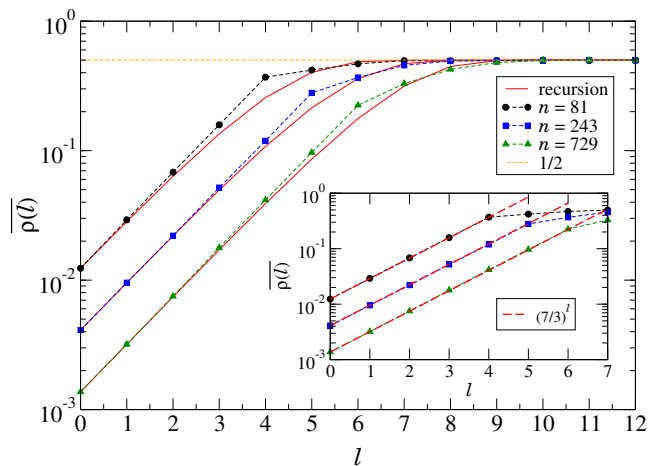


FIG. 4. Average density of NOT gates ($\hat{\sigma}^x$) as a function of the number, ℓ , of conjugation layers of inflationary gates for $n = 81, 243,$ and 729 (dashed lines are guides to the eye). The red lines indicate the recursion prediction, Eq. (52), with the initial condition $\rho(0) = 1/n$. The dashed-dotted line indicates the saturation value $1/2$. Averages are taken over 512 independent realizations of tree-structured circuits assembled by randomly and uniformly drawing from the 144 inflationary gates, and permuting the n bitlines, as described in Sec. VII A. Statistical error bars are too small to be discerned. The inset shows the agreement with the initial growth of the density scaling as $(7/3)^\ell$ (long dashed lines). Note also that the saturation at $\rho = 1/2$ after $\ell \sim \log_2 n$ layers predicted by the analytical mean field calculation is consistent with the qualitative argument given in the last paragraph of Sec. VI A. As expected, the deviations (at intermediate densities) of the numerical simulations from the mean-field prediction in Eq. (52) decrease as n increases.

Henceforth, we will fix the number of layers ℓ_{L_l} and ℓ_{L_r} of the inflationary stages \hat{L}_l and \hat{L}_r , respectively, of our cipher to be $\ell_{L_l} = \ell_{L_r} = \log_2 n$, which suffices to reach the saturation density $\rho = 1/2$ and, more importantly, will also lead to exponential decay (in n) of OTOCs, as shown below in Sec. VII D.

C. String proliferation with a tree-structured circuit

Here we exploit the tree-structured circuit to estimate the rate of string-entropy production as a function of the number of layers of super-nonlinear gates employed in \hat{N} . The conjugation of the macroscopic string $\hat{S}_{l(\alpha)}$ generated by inflation is carried out layer-by-layer, gate-by-gate of \hat{N} .

We proceed by determining the entropy produced via conjugation with one layer of super-nonlinear gates. Because of the macroscopic cross-section of inflated strings, every one of the $n/3$ super-nonlinear gates of the layer will produce, on average, entropy Δs . Averaging the entries for s_α in Table III over the sectors yields $\Delta s =$

$7/64 \times 2 \ln 2 + 28/64 \times 4 \ln 2 + 28/64 \times 4 \ln 2 \approx 2.58$. In turn, the total string-entropy produced by conjugation with the $n/3$ gates of one layer of \hat{N} is $S^N(1) \sim \Delta s \times \frac{n}{3}$.

Because of the hierarchical (tree-structured) wiring of the circuit, the entropy generated by conjugation with consecutive layers should be additive, and therefore the string-entropy after ℓ layers scales as $S^N(\ell) \sim S^N(1) \times \ell$, up to the point where $S^N(\ell)$ curves to account for the saturation to its maximum equilibrium value $S_1^{eq} = n \ln 4 - \Delta_1^{eq}$ (see Sec. V A). The linear scaling with ℓ allows us to conclude that producing the maximum extensive part of the entropy, $n \ln 4$, only requires $\mathcal{O}(1)$ layers, namely $\ell_s = 3 \ln 4 / \Delta s \approx 1.61$. It is the process of saturating the *sub-extensive* correction to its precise value Δ_1^{eq} that requires $\mathcal{O}(\log n)$ layers!

The circuit depth for saturation of the sub-extensive correction to the entropy can be determined from the following argument. Because of the tree-structure of the circuit, after $q-1$ layers, one can identify three independent subsystems that are not yet connected by super-nonlinear gates. The three disjoint subset of bits comprising these subsystems can be grouped according to the value of the most significant trit indexing bitlines [see Eq. (50)]. (It is not until layer $\ell = q$ that these three separate subsystems are connected by super-nonlinear gates.) The maximum entropy for the system that can be reached with $q-1$ layers is the sum of the saturation entropies of the three subsystems – additive because of separability – namely, $3 \times [(n/3) \ln 4 - \Delta_1^{eq}] = n \ln 4 - 3 \Delta_1^{eq}$, a value $2 \Delta_1^{eq}$ below the equilibrium entropy of the whole system. It then follows that, in order to eliminate this entropy deficit and saturate the entropy, including its sub-extensive universal correction of $\mathcal{O}(1)$, one needs at least the additional q th layer of super-nonlinear gates to bridge the three substructures and connect all $n = 3^q$ bits of the system. We conjecture that because of the extensive rate of entropy production per layer, once this bottleneck is eliminated by connecting across all degrees of freedom in the system, the full saturation of the entropy to its maximum is achieved.

We remark that the saturation of the entropy with the application of $\mathcal{O}(\log n)$ layers of super-nonlinear gates is consistent with the following observation. The degree of the Boolean polynomial functions representing individual output bits of a circuit built out of ℓ_N layers of nonlinear gates is at most 2^{ℓ_N} because 3-bit gates output are at most quadratic functions. Therefore, $\ell_N \sim \mathcal{O}(\log n)$ layers of nonlinear gates are required in order to reach pseudo-random permutations, for which individual outputs are polynomials of arbitrary order up to n . Generically, such Booleans are unlearnable in polynomial time.

D. SAC OTOC for the multi-stage cipher

The tree structure enables a calculation of the SAC OTOC, Eq. (6), which shows explicitly that the cipher

structured as in Fig. 3, with three stages each built out of $\log_2 n$ layers, suppresses the OTOC exponentially in n . The case of the SAC OTOC provides the simplest illustration of the mechanism by which the three-stage cipher is secure against differential attacks.

We compute the square of the SAC OTOC, $q^{ij} \equiv \left(C_{\text{SAC}}^{ij}\right)^2$, as a function of the number of applied layers of gates ℓ of the permutation associated with the operator \hat{P} in Eq. (45). The calculation, which is carried out in bit space, makes the mean-field assumption (checked *a posteriori* in a numerical simulation) that the system self-averages and $q^{ij} = q$, independent of i and j . We structure the calculation recursively, layer-by-layer, relating $q(\ell+1)$ to $q(\ell)$. We note that the recursion relation depends on the gate content (inflationary or super-nonlinear) of each layer.

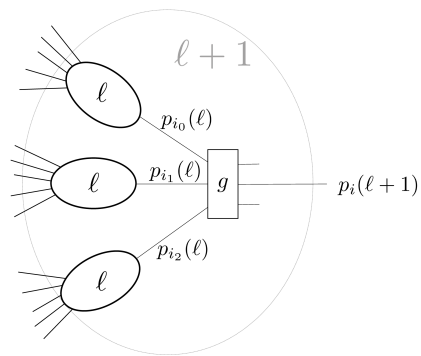


FIG. 5. The hierarchical structure of the circuit connectivity that illustrates the arguments used in the derivation of a recursion relation for the probability p_i that a bit flips upon flipping a number of inputs.

We proceed by defining $p_i(\ell)$ to be the fraction of all possible input states such that x_i^{out} remains put at x_i^{out} [as opposed to flipping to $\overline{x_i^{\text{out}}}$, with probability $1 - p_i(\ell)$] upon flipping a set of inputs of a system with ℓ layers. In the hierarchical tree construction, a given output bit i (at level $\ell+1$) is obtained by taking three outputs, at bitlines i_0, i_1, i_2 coming from separate branches of the tree (at level ℓ), as inputs to a 3-bit gate g that affects the output bit i (see Fig. 5). The specific action of the gate g determines the fraction of inputs for which the output i flips when $x \rightarrow x \oplus c$, with $x \equiv x_{i_0} + 2 x_{i_1} + 2^2 x_{i_2}$ and $c \equiv c_0 + 2 c_1 + 2^2 c_2$ encoding which ones of the three bits are flipped ($c_{0,1,2} = 0$ for an unflipped input or 1 for a flipped one). This fraction is expressed as a coefficient $C_{c_0 c_1 c_2}^{g_i} \equiv C_c^{g_i} = 2 f_c^{g_i} - 1$, with

$$f_c^{g_i} = \frac{1}{2^3} \sum_{x=0}^7 (-1)^{g_i(x) \oplus g_i(x \oplus c)}. \quad (54)$$

The recursion for the flipping probabilities can then be expressed as

$$\begin{aligned} p_i(\ell + 1) &= h(p_{i_0}(\ell), p_{i_1}(\ell), p_{i_2}(\ell); \{C_c^{g_i}\}) \\ &= p_{i_0}(\ell) p_{i_1}(\ell) p_{i_2}(\ell) C_{000}^{g_i} + (1 - p_{i_0}(\ell)) p_{i_1}(\ell) p_{i_2}(\ell) C_{100}^{g_i} + \cdots + (1 - p_{i_0}(\ell)) (1 - p_{i_1}(\ell)) (1 - p_{i_2}(\ell)) C_{111}^{g_i}. \end{aligned} \quad (55)$$

Note that Eq. (55) refers to a gate, g , which is part of a specific, given realization of a circuit. We now proceed to consider ensembles of circuits, and analyze the evolution of the probability distribution, $P(p_i; \ell)$, of the p_i , as function of ℓ . The recursion relation for $P(p_i; \ell)$ is obtained by using Eq. (55), and reads

$$P(p_i; \ell + 1) = \sum_{g \in S_8} \int dp_{i_0} dp_{i_1} dp_{i_2} P(p_{i_0}; \ell) P(p_{i_1}; \ell) P(p_{i_2}; \ell) \mathcal{P}_{\text{set}}(g) \delta[p_i - h(p_{i_0}, p_{i_1}, p_{i_2}; \{C_c^{g_i}\})], \quad (56)$$

where the gates are drawn from a probability distribution $\mathcal{P}_{\text{set}}(g)$, which depends on the gate set, and we assumed that the distribution P is independent of the bitline index i . The initial condition is determined by the fraction f ³ of bits that are flipped on input:

$$P(p; \ell = 0) = f \delta(p) + (1 - f) \delta(p - 1). \quad (57)$$

To see the evolution of the distribution and the vanishing of the SAC, we compute the average and moments of p . It is useful to change variables to $s_i(\ell) \equiv 2p_i(\ell + 1) - 1$, for which the recursion Eq. (55) reads

$$s_i(\ell + 1) = \tilde{C}_{100}^{g_i} s_{i_0}(\ell) + \tilde{C}_{010}^{g_i} s_{i_1}(\ell) + \tilde{C}_{001}^{g_i} s_{i_2}(\ell) + \cdots + \tilde{C}_{111}^{g_i} s_{i_0}(\ell) s_{i_1}(\ell) s_{i_2}(\ell), \quad (58)$$

with

$$\tilde{C}_a^{g_i} \equiv \frac{1}{2^3} \sum_{c=0}^7 (-1)^{a \cdot c} C_c^{g_i}, \quad (59)$$

where $a \cdot c \equiv a_0 c_0 + a_1 c_1 + a_2 c_2$.

These relations allow us to compute the evolution of the moments $\overline{s^q(\ell)}$. (Even if the distributions for the s_i are identical, independent of i , we keep some of the explicit indices for bookkeeping of contractions.) The average

$$\begin{aligned} \overline{s(\ell + 1)} &= \sum_{a=1}^7 \overline{\tilde{C}_a^{g_i}} \overline{[s_{i_0}(\ell)]^{a_0} [s_{i_1}(\ell)]^{a_1} [s_{i_2}(\ell)]^{a_2}} \\ &= \sum_{a=1}^7 \overline{\tilde{C}_a^{g_i}} \overline{[s(\ell)]^{a_0 + a_1 + a_2}}. \end{aligned} \quad (60)$$

The recursion relating $\overline{s(\ell + 1)}$ to $\overline{s(\ell)}$ depends on the gate set used for layer ℓ through the coefficients $\overline{\tilde{C}_a^{g_i}}$, which we present explicitly below for the cases of inflationary and super-nonlinear gates.

Similarly, we compute the second moment

$$\overline{s^2(\ell + 1)} = \sum_{a,b=1}^7 \overline{\tilde{C}_a^{g_i} \tilde{C}_b^{g_i}} \overline{[s_{i_0}(\ell)]^{a_0 + b_0} [s_{i_1}(\ell)]^{a_1 + b_1} [s_{i_2}(\ell)]^{a_2 + b_2}}. \quad (61)$$

We next consider explicitly the two classes of gates – inflationary and super-nonlinear gates – that are deployed in the three-stage cipher. For notational simplicity, we define the variables $s(\ell) \equiv \overline{s(\ell)}$ and $q(\ell) \equiv \overline{s^2(\ell)}$.

1. Inflationary layers

Upon computing the averages $\overline{\tilde{C}_a^{g_i}}$ and $\overline{\tilde{C}_a^{g_i} \tilde{C}_b^{g_i}}$ over the 144 inflationary gates, the recursion relations read

$$s(\ell + 1) = \frac{2}{3} [s(\ell)]^2 + \frac{1}{3} [s(\ell)]^3, \quad (62a)$$

³ We note that the assumption of independence of the bitline index cannot be justified unless f is intensive, which only occurs

through the action of sufficient number of layers of inflationary gates, see Fig. 4.

$$q(\ell + 1) = \frac{2}{3} [q(\ell)]^2 + \frac{1}{3} [q(\ell)]^3. \quad (62b)$$

The inflationary gates are special in that: (a) the equations for the averages and second moments decouple; and more importantly (b) there is no linear term in $q(\ell)$ in the equation for the second moment.

Note that the bimodal initial condition Eq. (57), where p only takes values $p = 0, 1$, implies that an initial $q = 1$ cannot evolve under Eq. (62b), which displays fixed points at $q = 0, 1$ (and a non-physical one at $q = -3$). Hence, the value of q cannot decay under the sole application of inflationary gates. However, once nonlinear gates are applied and q drops below 1, action by inflationary gates can accelerate its decay to zero because of the absence of the linear term in $q(\ell)$ in the recursion Eq. (62b).

2. Super nonlinear layers

Using the averages $\overline{C_a^{g_i}}$ and $\overline{C_a^{g_i} C_b^{g_i}}$ computed over the 10752 super-nonlinear gates, the corresponding recursion relations read

$$s(\ell + 1) = \frac{3}{7} s(\ell) + \frac{3}{7} [s(\ell)]^2 + \frac{1}{7} [s(\ell)]^3, \quad (63a)$$

$$q(\ell + 1) = \frac{3}{28} ([s(\ell)]^2 + [s(\ell)]^3) + \frac{3}{28} q(\ell) (1 + 2s(\ell) + 2[s(\ell)]^2) + \frac{3}{28} [q(\ell)]^2 (1 + s(\ell)) + \frac{1}{28} [q(\ell)]^3. \quad (63b)$$

By contrast to the case of the inflationary gates, the recursion relation for $q(\ell+1)$ above depends on both $s(\ell)$ and $q(\ell)$, and, more importantly, it does contain a term linear in $q(\ell)$. Note that, if the cipher only involved super-nonlinear gates, the decay of q would be at most exponential in ℓ because of the linear terms in $q(\ell)$. In this case, reaching values of q that are exponentially small in n would require $\mathcal{O}(n)$ layers. By contrast, as we show below, the cipher with two inflationary and one super-nonlinear stage reaches values of q that are exponentially small in n with no more than $\mathcal{O}(\log n)$ layers of gates for each stage.

3. Decay of SAC OTOC for the three-stage cipher

We proceed sequentially stage-by-stage.

1. First inflationary stage:

As shown in Sec. VII B, after $\ell_{L_i} = \log_2 n$ layers of gates an initial string grows to macroscopic weight, corresponding to a fraction $f \rightarrow 1/2$ in the initial condition for the recursions for the two subsequent stages, or equivalently, $s \rightarrow 0$.⁴

2. Super-nonlinear stage:

Taking $s \rightarrow 0$ simplifies the recursion relation for

the second stage to:

$$q(\ell + 1) = \frac{3}{28} q(\ell) + \frac{3}{28} [q(\ell)]^2 + \frac{1}{28} [q(\ell)]^3, \quad (64)$$

with ℓ in the range $\ell_{L_i} \leq \ell \leq \ell_{L_i} + \ell_N - 1$, and an initial condition $q(\ell_{L_i}) = 1$.

3. Final inflationary stage:

For the final stage, the recursion switches to:

$$q(\ell + 1) = \frac{2}{3} [q(\ell)]^2 + \frac{1}{3} [q(\ell)]^3, \quad (65)$$

with ℓ in the range $\ell_{L_i} + \ell_N \leq \ell \leq \ell_{L_i} + \ell_N + \ell_{L_r} - 1$. The condition used to initiate this last stage, $q(\ell_{L_i} + \ell_N)$, is the final result of the previous stage.

⁴ One can arrive at a similar scaling for the number of layers ℓ_{L_i} , but with a different prefactor, by deploying the recursion Eq. (62a) with an initial condition $s(0) = 1 - 2/n$, corresponding to a single flipped input. However, the recursion with this initial condition is not accurate because one cannot justify the assumption of independence of the bitline index. We therefore prefer to use the calculation of Sec. VII B to determine the depth ℓ_{L_i} needed to take $s \rightarrow 0$.

We can now examine the decay of the SAC OTOC from the final $q(\ell_{L_i} + \ell_N + \ell_{L_r})$ resulting from iterating these recursion relations. We shall place a bound on $q(\ell_{L_i} + \ell_N + \ell_{L_r})$ as follows.

First, by using the initial condition $q(\ell_{L_i}) = 1$ in Eq. (64), we obtain $q(\ell_{L_i} + 1) = 1/4$, which allows us to replace the recursion Eq. (64), for the subsequent steps with ℓ in the range $\ell_{L_i} + 1 \leq \ell \leq \ell_{L_i} + \ell_N - 1$, with the

inequality

$$\begin{aligned} q(\ell+1) &\leq \frac{3}{28}q(\ell) + \frac{3}{28} \times \frac{1}{4}q(\ell) + \frac{1}{28} \times \frac{1}{16}q(\ell) \\ &= \frac{61}{448}q(\ell). \end{aligned} \quad (66)$$

Thus, after ℓ_N layers of super-nonlinear gates we obtain $q(\ell_{L_i} + \ell_N) \leq \frac{1}{4} \left(\frac{61}{448}\right)^{\ell_N-1}$. This value is fed into the recursion for q for the final inflationary stage, Eq. (65), which can in turn be replaced by the inequality

$$q(\ell+1) \leq [q(\ell)]^2, \quad (67)$$

to be used in the range $\ell_{L_i} + \ell_N \leq \ell \leq \ell_{L_i} + \ell_N + \ell_{L_r} - 1$.

We thus arrive at the upper bound for the final value of q , after all $\ell_{L_i} + \ell_N + \ell_{L_r}$ layers of the three stages of the cipher, namely

$$q(\ell_{L_i} + \ell_N + \ell_{L_r}) \leq \left[\frac{1}{4} \left(\frac{61}{448} \right)^{\ell_N-1} \right]^{2^{\ell_{L_r}}}. \quad (68)$$

We remark that the expression above was derived by using a continuum mean-field approach, enabled by the tree structure of the cipher, which should break down once q drops below 2^{-n} – at that point, the action of the cipher can no longer be distinguished from that of a random permutation via the SAC OTOC, even if one has access to all the 2^n input/output relations. It follows from Eq. (68) and our arguments for the depth of the first inflationary layer above that $\ell_{L_i} = \ell_{L_r} = \log_2 n$ are sufficient to comfortably achieve this criterium. (Recall that $\ell_N = \log_3 n$ super-nonlinear layers are needed to saturate the entropy.)

The predictions of the recursions derived above are in excellent agreement with numerical simulation results shown in Fig. 6, which give us confidence in the intuition we have built on the basis of our analytical approach about the mechanisms responsible for the exponential (in n) decay of the OTOCs. This intuition is summarized by the inequality Eq. (68). Most notably, removing the last stage of inflationary gates would yield a q that decays exponentially with the number of layers, which only leads to polynomial in n decay with $\mathcal{O}(\log n)$ layers of nonlinear gates, and would instead require $\mathcal{O}(n)$ layers for exponential decay. The conclusion would be unchanged had we removed both inflationary stages, in which case the cipher would consist solely of nonlinear gates. (The decay of the q in this case is dominated by the tails in the stay-probability of small strings discussed above.) Also note that a single layer of super-nonlinear gates, when flanked by the two inflationary stages with $\mathcal{O}(\log n)$ layers, would be sufficient to suppress q exponentially in n . However, in this case the entropy (generated only by nonlinear gates), while extensive in n , would not saturate the equilibrium value, which we argued requires at least $\mathcal{O}(\log n)$ layers of nonlinear gates. This last example highlights that an OTOC can vanish exponentially while the output function is still learnable in polynomial time, as discussed in

Sec. VII C. In final analysis, this supports our conclusion that the criterium for pseudo-randomness must be that, up to an exponentially small fraction of atypical (exponentially hard to identify) cases, OTOCs must vanish, and the string entropies must saturate to their equilibrium values, including their non-extensive contributions.

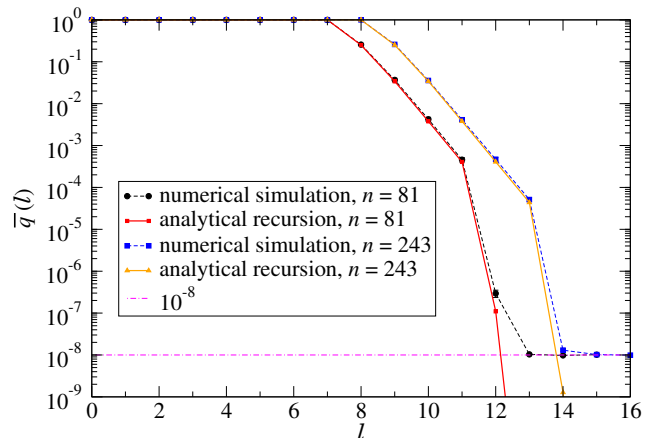


FIG. 6. Square of the SAC OTOC, computed as a function of the number of applied layers, ℓ , for three-stage ciphers with $\ell_{L_i} = \ell_{L_r} = \log_2 n$ and $\ell_N = \log_3 n$. The simulation is carried out for circuits with $n = 81$ and $n = 243$, and involves: (i) averaging over 56 ($n = 81$) and 32 ($n = 243$) random and independent circuit realizations of the three-stage cipher; and (ii) sampling over $M = 10^8$ input states selected randomly from the 2^n possible inputs. The numerical data points (dashed lines are guides to the eye) are compared to the predictions from the analytical recursion relations (shown as solid lines). The numerical results can only capture the behavior down to the floor level of $M^{-1} = 10^{-8}$ (indicated by the horizontal dash-dotted line). Note that, consistent with analytical predictions, $q(\ell)$: (i) remains constant, equal to 1, throughout the first stage of inflation; (ii) decays approximately exponentially in ℓ after the first super-nonlinear layer; and (iii) drops faster than exponential in ℓ as soon as the last linear stage becomes active. Also notice that the double-exponential decay of q with ℓ , predicted for this last stage, is difficult to capture with numerical simulation, and equally difficult to ascertain by an adversary with polynomial resources.

VIII. CONCLUSIONS AND OPEN DIRECTIONS

In this paper we presented a framework for analysis and design of classical ciphers based on a close conceptual connection to the problem of scrambling of quantum states. The close parallels to quantum problems emerge naturally when we translate the actions of measuring or flipping bits describing cipher attacks to Pauli string operators. It is in string space that quantum mechanical-like concepts, such as superposition of states and operator spreading, become manifest. Here we studied the evolution of a classical computation in string space and connected measures of cipher security, such as resistance to

plaintext and ciphertext attacks, to the vanishing of out-of-time-order correlators (OTOCs), which in quantum systems characterizes the appearance of chaos. Starting from any initial string state, in both classical and quantum random circuits, scrambling and chaos follow from the delocalization of amplitudes across the exponentially large Hilbert space of string states. We quantified this delocalization in string space in terms of participation ratios and associated entropies. We argued that, in order for a cipher to be indistinguishable from a random permutation via polynomial number of queries, the OTOCs must vanish super-polynomially in the number of bits and string entropies must saturate. An important conclusion of this paper is that, for random tree-structured three-stage ciphers built out of 3-bit gates in S_8 , OTOCs vanish exponentially and string entropies saturate for circuits with as few as $\mathcal{O}(n \ln n)$ gates.

In order to reach this result we had to circumvent the effect of rare events and the associated tails in the distribution of string weights, connected with the slow growth of initially small strings. The same problem appears in the analysis of scrambling by random quantum circuits, in which case overcoming these tails requires larger circuits. In particular, Brown and Fawzi [19, 20] prove scrambling and decoupling for circuits with $\mathcal{O}(n \ln^2 n)$ gates, and Harrow and Mehraban [22] prove that circuits laid down in $D \sim \ln n$ dimensional lattices would scramble with $\mathcal{O}(n \ln n \ln \ln n)$ gates. (Ref. [22] also conjectures that one should be able to achieve scrambling with $\mathcal{O}(n \ln n)$ gates, as we argued here.) The insight that allows us to establish our result for the shorter circuit is to separate two distinct processes controlling the evolution of string wave function amplitudes, which we apply sequentially in a three-stage structure. The first and the third circuits of the structure involve the extension of small weight strings in the initial and final states to strings of macroscopic weight (of order $3n/4$), processes implemented via a set of 144 special linear gates (out of the 8! gates in S_8). These “inflationary” gates have the property that the stay-probability for weight 1 substrings vanishes, ensuring that strings gain weight at a sufficiently fast rate that the tails decay exponentially with n already for a circuit with $\mathcal{O}(n \ln n)$ gates. The second process, implemented by the middle layer of the cipher (bookended by the two inflationary stages) involves applying “super-nonlinear” gates to heavy strings emerging from the inflationary periods. During this string “proliferation” stage, the application of a nonlinear gate splits a string state into a superposition of multiple heavy string states, rapidly leading to an exponential number of non-zero string amplitudes. As discussed in the text, it is this proliferation in string space that leads to the maximum entropies defined from the string state probabilities and to the vanishing of OTOCs characterizing scrambling.

We reiterate that the diagnostics for the quality of a classical cipher advanced in this paper are (i) the vanishing of OTOCs which describe arbitrary (higher-order) differential attacks; and (ii) the saturation of the

string entropy. Even if an adversary cannot compute the entropy for a specific permutation with polynomial resources (as the dimension of string space is exponential), our statistical mechanics approach allowed us to argue that the saturation of the n -independent $\mathcal{O}(1)$ deficit in Eq. (33) requires at least $\mathcal{O}(\log n)$ layers of super-nonlinear gates. As already mentioned in subsection VII C, this implies that the nonlinear Boolean functions expressing the outputs of our three-stage cipher following the action of $\ell_N \sim \mathcal{O}(\log n)$ layers of super-nonlinear gates have degrees of up to 2^{ℓ_N} . There are $\mathcal{O}(2^{2^{\ell_N}})$ coefficients in these polynomials, making it impossible to learn these functions via fitting with polynomial resources, another consistency argument for the security of our cipher. This should be contrasted with the situation of a cipher with a $\mathcal{O}(1)$ layers of nonlinear gates, which already saturates the extensive part of the entropy (but not its non-extensive correction), and generates polynomials of finite order that can be learned with polynomial resources.

We end with comments on three issues that may inspire future work. First, the three-stage structure that we employed in the context of the classical cipher can also be implemented in a tree-structured long-range quantum circuit, in which case we expect that reaching the random Haar measure can also be realized in a circuit with $\mathcal{O}(n \ln n)$ gates. It is already clear that this can be achieved if one uses the same 144 linear 3-bit (or 3-qubit) inflationary gates used above. We note that such a circuit would scramble in depth (or time) $\mathcal{O}(\ln n)$, matching the scrambling rate of a black hole [8–10, 12, 24, 25]. The remaining question is whether there is a random unstructured circuit of 2-qubit gates that can reach the same goal.

The second comment refers to the issue of averaging over circuits, which also connects to discussions of t -design (see [22, 33] and references therein). It is most instructive to consider an explicit example, namely that of the OTOC presented in Eq. (6), which measures the avalanche effect. For a given linear circuit [implemented by a linear permutation, $P_j(x \oplus 2^i) = P_j(x) \oplus P_j(2^i) \oplus b_j$, where $b_j = 0, 1$], $C_{\text{SAC}}^{ij} = (-1)^{P_j(2^i) \oplus b_j} = \pm 1$. For a *single* realization of a random circuit, the ± 1 value of the correlator signals a weak cipher. By contrast, as discussed above, a good cipher must be built out of nonlinear gates, in which case the correlator C_{SAC}^{ij} vanishes for a given (sufficiently large) circuit. It becomes immediately clear that if one averages over circuits at this stage, the difference between the linear and nonlinear circuits is washed out. This points to the dangers of averaging too early, an issue well known from the theory of spin glasses [34, 35]. Learning from the latter, one should consider the behavior of a *typical* circuit by first squaring the correlator and only then averaging. This suggests an Edwards-Anderson-like order parameter, $q_{\text{SAC}}^{ij} = \overline{(C_{\text{SAC}}^{ij})^2}$, which is equal to 1 for linear circuits and vanishes for good ciphers. One can repeat this

discussion in the context of quantum circuits, where averaging too early washes out the difference between Clifford and universal unitary gates. The vanishing of the average of the correlator C_{SAC}^{ij} is used to qualify Clifford circuits as 2-designs, a designation that is physically meaningless as it does not help one understand the behavior of a *typical* circuit. The difference between Clifford and universal quantum circuits becomes apparent if one uses the appropriate Edwards-Anderson-like order parameter, which in the language of t -designs requires correlators with $t \geq 4$.

A related point, which follows from the discussions of delocalization of wave function amplitudes in string space, is that once the system is delocalized as signaled by the inverse participation ratio in Eq. (25), it is delocalized by any other measure: “Delocalized systems are all alike; every localized system is localized in its own way.” This suggests that once a system is a 4-design, it is also a t -design for $t > 4$.

The third and final comment is that one can extend the discussion of classical attacks expressed as OTOCs to quantum attacks [26]. In the latter, the trace involved in the computation of correlation functions (OTOCs) is replaced by projective measurements following the action

of certain operations that can be translated into out-of-time-order operators (OTOOs), which we plan to explore in a future publication.

In closing, fast ciphers with circuits of depth $\mathcal{O}(\ln n)$ are intellectually interesting in their own right, as they saturate the speed limit of information scrambling [8–10, 12, 24, 25]. Of greater practical importance, however, is that they enable a polynomial-overhead framework – Encrypted-Operator Encryption – for secure computation directly on encrypted data, which we introduce in Ref. [14] as an alternative to Homomorphic Encryption [13].

ACKNOWLEDGMENTS

The authors would like to thank Shiyu Zhou and Luowen Qian for useful discussions at the early stages of this paper, and Ran Canetti for many enlightening conversations and for stimulating us to explore physics-inspired frameworks for quantifying scrambling by classical ciphers. We also acknowledge David Huse and Zhi-Cheng Yang for insightful discussions.

Appendix A: Derivation of the OTOC in Eq. (7) that is associated to a CPCA on a 3-round Feistel cipher

Here we translate the attack presented by Patarin [16] on a 3-round Feistel cipher [see Sec. VB, in particular Eqs. (35) and (36), for notation] into an OTOC. The attack requires 3 oracle queries, 2 queries to the encryption oracle, P , and 1 query to the decryption oracle, P^{-1} :

1. Choose an input $(L_0^{(1)}, R_0^{(1)})$ and ask the encryption oracle for the output $(L_3^{(1)}, R_3^{(1)}) = P(L_0^{(1)}, R_0^{(1)})$;
2. Choose $L_0^{(2)} \neq L_0^{(1)}$ but reuse the same $R_0^{(1)}$ value, and ask the encryption oracle for the output $(L_3^{(2)}, R_3^{(2)}) = P(L_0^{(2)}, R_0^{(1)})$;
3. Ask the decryption oracle for $(L_0^{(3)}, R_0^{(3)}) = P^{-1}(L_3^{(2)}, R_3^{(2)} \oplus L_0^{(1)} \oplus L_0^{(2)})$.

For $r = 3$, one can show using Eqs. (35, 36) that $R_0^{(3)} \oplus R_0^{(1)} \oplus L_3^{(2)} \oplus L_3^{(1)} = 0$.

To construct an OTOC that expresses the above constraint, it suffices to use one bit, i , of the R register and one bit, j , of the L register. The correlation

$$\begin{aligned} C_{\text{CPCA}}^{ij} &= \text{tr} [\rho_\infty \hat{\sigma}_j^x(0) \hat{\sigma}_i^x(\tau) \hat{\sigma}_i^z(0) \hat{\sigma}_i^x(\tau) \hat{\sigma}_j^z(\tau) \hat{\sigma}_j^x(0) \hat{\sigma}_j^z(\tau) \hat{\sigma}_i^z(0)] \\ &= (-1)^{\delta_{ij}} \text{tr} \left[\rho_\infty (\hat{\sigma}_i^z(0) \hat{\sigma}_i^x(\tau))^2 (\hat{\sigma}_j^z(\tau) \hat{\sigma}_j^x(0))^2 \right]. \end{aligned} \quad (\text{A1})$$

equals 1 if the evolution of the bit state is carried out via P and P^{-1} . The correspondence between the attack and the OTOC is extracted by following the sequence of operators from right-to-left in the first line of Eq. (A1):

1. $\hat{\sigma}_i^z(0)$ measures bit i of x_i , or equivalently bit $i - n/2$ of $R_0^{(1)}$ (R occupies the second half of the n -bit long block), through $(-1)^{x_i}$, at the initial input state, $|x\rangle = |(L_0^{(1)}, R_0^{(1)})\rangle$;
2. $\hat{\sigma}_j^z(\tau)$ measures bit j of $L_3^{(1)}$, through $(-1)^{P_j(x)}$, at the output and returns the system to the initial input state, $|x\rangle$;
3. $\hat{\sigma}_j^x(0)$ flips the j -th bit of the initial input state, $|x\rangle$, into $|x \oplus 2^j\rangle$, thus setting $L_0^{(2)} = L_0^{(1)} \oplus 2^j$;

4. $\hat{\sigma}_i^x(\tau)$ $\hat{\sigma}_j^z(\tau)$ first measures bit j of $L_3^{(2)}$, $(-1)^{P_j(x \oplus 2^j)}$, at the output, then flips the i -th of the output state, thus shifting $R_3^{(2)} \rightarrow R_3^{(2)} \oplus 2^{i-n/2}$, and subsequently evolves the system backwards (via the P^{-1}) to the state $|(L_0^{(3)}, R_0^{(3)})\rangle$;
5. $\hat{\sigma}_i^z(0)$ measures bit $i - n/2$ of $R_0^{(3)}$; and finally,
6. the product $\hat{\sigma}_j^x(0) \hat{\sigma}_i^x(\tau)$ undoes the flips above to restore the state to $|x\rangle$, so as to express the result as a trace over all possible inputs.

The correlator Eq. (A1) thus returns the average over inputs of $(-1)^{[R_0^{(3)}]_{i-n/2} + [R_0^{(1)}]_{i-n/2} + [L_3^{(2)}]_j + [L_3^{(1)}]_j}$; given the condition that $R_0^{(3)} \oplus R_0^{(1)} \oplus L_3^{(2)} \oplus L_3^{(1)} = 0$ for a 3-round Feistel cipher, it follows that

$$C_{\text{CPCA}}^{i=j+n/2} = 1. \quad (\text{A2})$$

We have therefore successfully translated the attack on the 3-round Feistel cipher in Ref. [16] into an OTOC.

Appendix B: Inflationary gates

In the table below we list all the permutations in S_8 that are associated to the 144 inflationary gates. These 3-bit gates are all linear, and can be expressed in a circuit equivalent with 2-bit CNOT gates as exemplified in Fig. B.1.

1: 03567421	25: 14637205	49: 25701643	73: 41273650	97: 52340761	121: 63145027
2: 03657412	26: 14726305	50: 25704316	74: 41362750	98: 52346107	122: 63501427
3: 03745621	27: 16254370	51: 27145063	75: 41367205	99: 52610734	123: 65031274
4: 03746512	28: 16257043	52: 27415036	76: 41723605	100: 52613407	124: 65120374
5: 05367241	29: 16432570	53: 27501463	77: 42173560	101: 53062471	125: 65123047
6: 05637214	30: 16437025	54: 27504136	78: 42351760	102: 53240671	126: 65301247
7: 05723641	31: 16702543	55: 30475621	79: 42357106	103: 53246017	127: 70162543
8: 05726314	32: 16704325	56: 30476512	80: 42713506	104: 53602417	128: 70164325
9: 06357142	33: 17246053	57: 30564721	81: 43162570	105: 56032174	129: 70251643
10: 06537124	34: 17426035	58: 30654712	82: 43167025	106: 56210374	130: 70254316
11: 06713542	35: 17602453	59: 34075261	83: 43251670	107: 56213047	131: 70431625
12: 06715324	36: 17604235	60: 34076152	84: 43257016	108: 56302147	132: 70432516
13: 07345261	37: 21475630	61: 34520761	85: 43701625	109: 60173542	133: 71062453
14: 07346152	38: 21564730	62: 34526107	86: 43702516	110: 60175324	134: 71064235
15: 07523461	39: 21567403	63: 34610752	87: 47123065	111: 60351742	135: 71240653
16: 07526134	40: 21745603	64: 34615207	88: 47213056	112: 60531724	136: 71420635
17: 07613452	41: 24175360	65: 35064271	89: 47301265	113: 61073452	137: 72051463
18: 07615234	42: 24531760	66: 35420671	90: 47302156	114: 61075234	138: 72054136
19: 12476530	43: 24537106	67: 35426017	91: 50273641	115: 61340752	139: 72140563
20: 12654730	44: 24715306	68: 35604217	92: 50276314	116: 61345207	140: 72410536
21: 12657403	45: 25164370	69: 36054172	93: 50362741	117: 61520734	141: 74031265
22: 12746503	46: 25167043	70: 36410572	94: 50632714	118: 61523407	142: 74032156
23: 14276350	47: 25431670	71: 36415027	95: 52073461	119: 63051472	143: 74120365
24: 14632750	48: 25437016	72: 36504127	96: 52076134	120: 63140572	144: 74210356

TABLE OF INFLATIONARY GATES. The lists of 8 numbers correspond to the outputs for each of the inputs 0 1 2 3 4 5 6 7, i.e., the corresponding permutation list. These 144 gates are found as follows. We compute the entries $t_{\alpha'\alpha}^{(g)}$ of the 64×64 transition in Eq. (41) for each of the $8!$ gates in S_8 . We filter out all gates for which the 9×9 submatrix connecting the 9-dimensional subspace of weight 1 strings is non-zero, thus retaining only gates for which weight 1 substrings grow into weight 2 or 3 substrings. All these gates are linear.

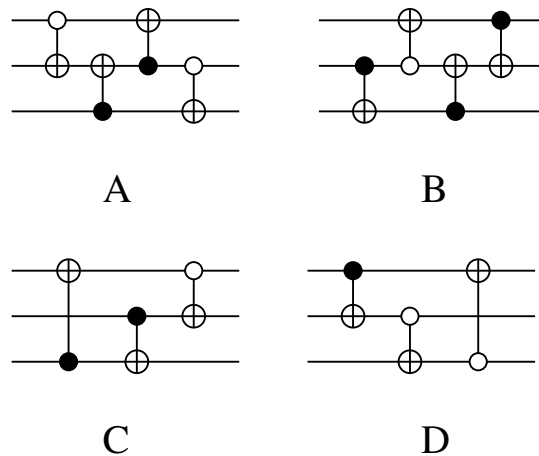


FIG. B.1. Examples of 4 circuits written with 2-bit CNOT gates that are equivalent to the inflationary 3-bit gates. There are $3 \times 2^{4-1} = 24$ circuits with the topology of the example shown in A, where the factor of 3 counts the number of ways of choosing the bit line with two controls, the factor of 2^4 counts the choices of negated or not control (white or black control), and the factor of 2^{-1} accounts for the fact that exchanging the color on the controls of the two gates with the targets on the same bitline does not change functionality of the assembly of the four CNOTs. Similarly, there are $3 \times 2^{4-1} = 24$ circuits with the topology of B. Finally, there are $3! \times 2^3 = 48$ circuits similar to C and $3! \times 2^3 = 48$ similar to D. In total, there are 144 such circuits.

-
- [1] S. Goldwasser and M. Bellare, “Lecture notes on cryptography,” Chap. 4, (2001).
- [2] Michael Luby and Charles Rackoff, “How to construct pseudorandom permutations from pseudorandom functions,” *SIAM Journal on Computing* **17**, 373–386 (1988), <https://doi.org/10.1137/0217022>.
- [3] Don Coppersmith and Edna Grossman, “Generators for certain alternating groups with applications to cryptography,” *SIAM Journal on Applied Mathematics* **29**, 624–627 (1975).
- [4] Shlomo Hoory, Avner Magen, Steven Myers, and Charles Rackoff, “Simple permutations mix well,” *Theoretical Computer Science* **348**, 251–261 (2005).
- [5] A. Brodsky and S. Hoory, “Simple permutations mix even better,” *Random Struct. Algorithms* **32**, 274–289 (2008).
- [6] A. I. Larkin and Yu. N. Ovchinnikov, “Quasiclassical method in the theory of superconductivity,” *Soviet Journal of Experimental and Theoretical Physics* **28**, 1200 (1969).
- [7] A Kitaev, “Hidden Correlations in the Hawking Radiation and Thermal Noise, talk given at KITP, Santa Barbara,” <http://online.kitp.ucsb.edu/online/joint98/kitaev/> (2014).
- [8] Stephen H. Shenker and Douglas Stanford, “Black holes and the butterfly effect,” *Journal of High Energy Physics* **2014** (2014), 10.1007/jhep03(2014)067.
- [9] Stephen H. Shenker and Douglas Stanford, “Multiple shocks,” *Journal of High Energy Physics* **2014** (2014), 10.1007/jhep12(2014)046.
- [10] Juan Maldacena, Stephen H. Shenker, and Douglas Stanford, “A bound on chaos,” *Journal of High Energy Physics* **2016** (2016), 10.1007/jhep08(2016)106.
- [11] Igor L. Aleiner, Lara Faoro, and Lev B. Ioffe, “Microscopic model of quantum butterfly effect: Out-of-time-order correlators and traveling combustion waves,” *Annals of Physics* **375**, 378 – 406 (2016).
- [12] Douglas Stanford, “Many-body chaos at weak coupling,” *Journal of High Energy Physics* **2016** (2016), 10.1007/jhep10(2016)009.
- [13] Robert Frederick, “Core concept: Homomorphic encryption,” *PNAS* **112**, 8515–8516 (2015).
- [14] Claudio Chamon, Jonathan Jakes-Schauer, Eduardo R. Mucciolo, and Andrei E. Ruckenstein, “Encrypted Operator Computing: an alternative to Fully Homomorphic Encryption,” unpublished.
- [15] F. Wegner, “Inverse participation ratio in $2+\epsilon$ dimensions,” *Zeitschrift für Physik B Condensed Matter and Quanta* **36**, 209–214 (1980).
- [16] Jacques Patarin, “Generic attacks on Feistel schemes,” in *Advances in Cryptology — ASIACRYPT 2001*, edited by Colin Boyd (Springer Berlin Heidelberg, Berlin, Heidelberg, 2001) pp. 222–238.
- [17] R. Oliveira, O. C. O. Dahlsten, and M. B. Plenio, “Generic entanglement can be generated efficiently,” *Physical Review Letters* **98** (2007), 10.1103/physrevlett.98.130502.
- [18] Aram W. Harrow and Richard A. Low, “Random quantum circuits are approximate 2-designs,” *Communications in Mathematical Physics* **291**, 257–302 (2009).
- [19] Winton Brown and Omar Fawzi, “Scrambling speed of random quantum circuits,” (2013), arXiv:1210.6644 [quant-ph].
- [20] Winton Brown and Omar Fawzi, “Decoupling with random quantum circuits,” *Communications in Mathematical Physics* **340**, 867–900 (2015).
- [21] Fernando G. S. L. Brandão, Aram W. Harrow, and Michał Horodecki, “Local random quantum circuits are approximate polynomial-designs,” *Communications in*

- Mathematical Physics **346**, 397–434 (2016).
- [22] Aram Harrow and Saeed Mehraban, “Approximate unitary t -designs by short random quantum circuits using nearest-neighbor and long-range gates,” (2018), arXiv:1809.06957 [quant-ph].
- [23] F. Arute, K. Arya, R. Babbush, D. Bacon, J. C. Bardin, R. Barends, R. Biswas, S. Boixo, F. G. S. L. Brandao, D. A. Buell, B. Burkett, Y. Chen, Z. Chen, B. Chiaro, R. Collins, W. Courtney, A. Dunsworth, E. Farhi, B. Foxen, A. Fowler, C. Gidney, M. Giustina, R. Graff, K. Guerin, S. Habegger, M. P. Harrigan, M. J. Hartmann, A. Ho, M. Hoffmann, T. Huang, T. S. Humble, S. V. Isakov, E. Jeffrey, Z. Jiang, D. Kafri, K. Kechedzhi, J. Kelly, P. V. Klimov, S. Knysh, A. Korotkov, F. Kostritsa, D. Landhuis, M. Lindmark, E. Lucero, D. Lyakh, S. Mandrà, J. R. McClean, M. McEwen, A. Megrant, X. Mi, K. Michielsen, M. Mohseni, J. Mutus, O. Naaman, M. Neeley, C. Neill, M. Yuezhen Niu, E. Ostby, A. Petukhov, J. C. Platt, C. Quintana, E. G. Rieffel, P. Roushan, N. C. Rubin, D. Sank, K. J. Satzinger, V. Smelyanskiy, K. J. Sung, M. D. Trevithick, A. Vainsencher, B. Villalonga, T. White, Z. Jamie Yao, P. Yeh, A. Zalcman, H. Neven, and J. M. Martinis, “Quantum supremacy using a programmable superconducting processor,” *Nature* **574**, 505–510 (2019).
- [24] Patrick Hayden and John Preskill, “Black holes as mirrors: quantum information in random subsystems,” *Journal of High Energy Physics* **2007**, 120–120 (2007).
- [25] Yasuhiro Sekino and L Susskind, “Fast scramblers,” *Journal of High Energy Physics* **2008**, 065–065 (2008).
- [26] Gembu Ito, Akinori Hosoyamada, Ryutaroh Matsumoto, Yu Sasaki, and Tetsu Iwata, “Quantum chosen-ciphertext attacks against feistel ciphers,” in *Topics in Cryptology – CT-RSA 2019*, edited by Mitsuru Matsui (Springer International Publishing, Cham, 2019) pp. 391–411.
- [27] Edward Fredkin and Tommaso Toffoli, “Conservative logic,” *International Journal of Theoretical Physics* **21**, 219–253 (1982).
- [28] Horst Feistel, “Cryptography and computer privacy,” *Scientific American* **228**, 15–23 (1973).
- [29] Sheelagh Lloyd, “Eurocrypt 90: Proceedings of the workshop on the theory and application of cryptographic techniques on advances in cryptology,” (Springer-Verlag, Berlin, Heidelberg, 1991).
- [30] Hirose Shouichi and Ikeda Katsuo, “Nonlinearity criteria of boolean functions,” (1995).
- [31] Daniel Gottesman, “The Heisenberg Representation of Quantum Computers,” in *Proceedings of the XXII International Colloquium on Group Theoretical Methods in Physics*, eds. S. P. Corney, R. Delbourgo, and P. D. Jarvis (International Press, 1999) pp. 32–43.
- [32] Scott Aaronson and Daniel Gottesman, “Improved simulation of stabilizer circuits,” *Physical Review A* **70** (2004), 10.1103/physreva.70.052328.
- [33] Daniel A. Roberts and Beni Yoshida, “Chaos and complexity by design,” *Journal of High Energy Physics* **2017** (2017), 10.1007/jhep04(2017)121.
- [34] K. H. Fischer and J. A. Hertz, *Spin glasses*, 1st ed., Cambridge Studies in Magnetism (Cambridge Univ. Press, Cambridge, 1993).
- [35] S F Edwards and P W Anderson, “Theory of spin glasses,” *Journal of Physics F: Metal Physics* **5**, 965–974 (1975).